Elsevier Editorial System(tm) for Journal of Cleaner Production

Manuscript Draft

Manuscript Number:

Title: Tunable Cu-hydrotalcite derived mixed oxides for sustainable ethanol condensation to n-butanol in liquid phase

Article Type: Original article

Keywords: n-butanol; ethanol condensation; Cu-hydrotalcite; copper content; liquid phase.

Corresponding Author: Professor Anna Maria Raspolli galletti, Ph.D.

Corresponding Author's Institution: University of pisa

First Author: Anna Maria Raspolli galletti, Ph.D.

Order of Authors: Anna Maria Raspolli galletti, Ph.D.; Patricia Benito; Angelo Vaccari; Claudia Antonetti; Domenico Licursi; nicola Schiaroli; Enrique Rodriguez-Castellon

Abstract: 1-Butanol (BuOH) is a renewable molecule largely employed as solvent and green fuel additive, in order to reduce the fossil fuel depletion. The synthesis of BuOH has now been performed by condensation of ethanol, carried out in liquid phase in the presence of Cu/Mg/Al hydrotalcite-derived mixed oxides. Different Cu/Mg/Al mixed oxides catalysts, with Cu atomic content in the range 7.6-1.0 %, were synthesized, characterized and tested in the condensation runs carried out at temperatures 215-230 °C. Tailoring Cu-content in hydrotalcite-derived Cu/Mg/Al mixed oxides allowed to address the Guerbet reaction towards BuOH formation, highlighting how a low Cu-content favours the condensation to butanol and higher alcohols, while decreasing the ester formation. For the first time, appreciable performances (conversion up to 32.0 mol % with a selectivity to BuOH of 53 mol%) were ascertained in a batch process carried out under subcritical conditions. The obtained performances were enhanced by removing the co-produced water which caused the reconstruction of the hydrotalcite structure. Extensive characterizations (such as B.E.T., powder XRD, H2-TPR, CO2 TPD, HRTEM, XPS, ICPS) of precursors and of calcined, pre-reduced and spent catalysts were carried out in order to establish structure-performance trends.

Suggested Reviewers: Vicente Rives Full professor
University of Salamanca
vrives@usal.es
Leading researcher on sustainable catalysis for cleaner processes

Guido Busca
Full professor, University of Genova
Guido.Busca@unige.it
Outstandng scientist in the field of catalysis for sustainable processes, in particular heterogeneous catalysis

Jun Ni
University of Technology, Hangzhou

junni@zjut.edu.cn
Recent reviewer in the field of ethanol condensation for butanol production

An Verberckmoes
University of Gent
An.Verberckmoes@UGent.be
Leading experience on cleaner catalytic processes and on ethanol condensation

**WORDS (manuscript, Tables, Figures and Scheme):7990**

# Tunable Cu-hydrotalcite derived mixed oxides for sustainable ethanol condensation to n-butanol in liquid phase

Patricia Benito[a*], Angelo Vaccari[a], Claudia Antonetti[b], Domenico Licursi[b], Nicola Schiarioli[a], Enrique Rodriguez-Castellón[c], Anna Maria Raspolli Galletti[b]*

[a]Dipartimento di Chimica Industriale "Toso Montanari", Università di Bologna, Viale Risorgimento 4, 40136, Bologna, Italy.

[b]Dipartimento di Chimica e Chimica Industriale, Università di Pisa, Via G. Moruzzi 13, 56124 Pisa, Italy.

[c]Departamento de Química Inorgánica, Facultad de Ciencias, Universidad de Málaga, 29071 Málaga, Spain

**Abstract**

1-Butanol (BuOH) is a renewable molecule largely employed as solvent and green fuel additive, in order to reduce the fossil fuel depletion. The synthesis of BuOH has now been performed by condensation of ethanol, carried out in liquid phase in the presence of Cu/Mg/Al hydrotalcite-derived mixed oxides. Different Cu/Mg/Al mixed oxides catalysts, with Cu atomic content in the range 7.6-1.0 %, were synthesized, characterized and tested in the condensation runs carried out at temperatures 215-230 °C. Tailoring Cu-content in hydrotalcite-derived Cu/Mg/Al mixed oxides allowed to address the Guerbet reaction towards BuOH formation, highlighting how a low Cu-content favours the condensation to butanol and higher alcohols, while decreasing the ester formation. For the first time, appreciable performances (conversion up to 32.0 mol % with a selectivity to BuOH of 53 mol%) were ascertained in a batch process carried out under subcritical conditions. The obtained performances were enhanced by removing the co-produced water which caused the reconstruction of the hydrotalcite structure. Extensive characterizations (such as B.E.T., powder XRD, $H_2$-TPR, $CO_2$ TPD, HRTEM, XPS, ICPS) of precursors and of calcined, pre-reduced and spent catalysts were carried out in order to establish structure-performance trends.

**Keywords:** *n*-butanol; ethanol condensation; Cu-hydrotalcite; copper content; liquid phase.

*Corresponding authors, e-mail: patricia.benito3@unibo.it; anna.maria.raspolli.galletti@unipi.it.

## 1. Introduction

Bioethanol (EtOH) is largely employed as solvent and as a green fuel additive, with the aim of reducing the fossil fuel depletion and environmental issues. The use of ethanol-blended gasoline is increasing, but the EtOH content must be maintained below 20 wt % due to the many drawbacks, such as its high volatility, high hydrophilicity and lower energy content compared to gasoline (Britto Júnior and Martins, 2015). On the other hand, 1-butanol (BuOH) represents a valuable alternative as fuel additive, due to its physic-chemical properties which are more similar to those of gasoline (Pereira et al., 2015; Singh et al., 2015). Therefore, the increasing availability of bioethanol makes extremely interesting its Guerbet condensation to 1-butanol (Wu et al., 2018; Li, H. et al., 2018; Zaccheria et al., 2018; Zhang et al., 2016). The Guerbet reaction is a catalytic strategy for upgrading lower alcohols to give valuable chemicals and energy-intensive fuels and involves the condensation of two alcohols to give a β-alkylated dimer alcohol, with the concomitant release of water. This condensation is generally reported to proceed by five successive steps (Scheme 1): 1) dehydrogenation of the starting alcohols to give the corresponding aldehydes; 2) aldol condensation of the aldehydes; 3) dehydration; and 4-5) final hydrogenations of the unsaturated aldol condensation products to give the higher Guerbet alcohols (Gabriëls et al., 2015; Kozlowski and Davis, 2013).

Scheme 1, near here

The dehydrogenation (Step 1) is endothermic, thermodynamically favoured at high temperatures, and often reported as the rate limiting step, in particular when lower alcohols are employed as substrates in the liquid phase (Dowson et al., 2013). In order to improve the dehydrogenation and the successive hydrogenation steps, the presence of a transition metal in the catalytic system can be crucial. On the other hand, the aldol condensation (Step 2) is catalyzed by basic, acidic or amphoteric catalysts and is thermodynamically unfavorable, whilst the successive aldol dehydration to give the α,β-unsaturated aldehyde (Step 3) is highly favorable and shifts the overall reaction. Many authors have reported the negative effect of the co-produced water on the reaction behavior, in particular working in the liquid phase (Marcu et al., 2009; Riittonen et al., 2012, 2014; Sreekumar et al., 2014). Finally the hydrogenation reactions (Steps 4 and 5) are favored by low temperatures. The above mechanism is largely accepted as the effective one at low temperatures (in

particular in the liquid phase) and in the presence of hydrogenating/dehydrogenating catalytic components. For the Guerbet condensation of ethanol to BuOH in the presence of purely basic heterogeneous catalysts, which is performed in the gas phase at high temperatures (generally above 400 °C), also direct condensation mechanisms have been proposed (Chieregato et al., 2015; Meunier et al., 2015). In the past we studied the Guerbet reaction for obtaining isobutanol from mixtures of methanol (MeOH) and n-propanol (PrOH) (Carlini et al., 2003a, 2003b, 2003c, 2002), adopting sodium alkoxide as homogeneous basic component and different homogeneous or heterogeneous metal components based on Cu, Ni, Pd or Rh. However, the use of the homogeneous sodium alkoxide gave serious drawbacks and completely heterogeneous Cu-based bifunctional catalysts were then adopted for MeOH/PrOH condensation, testing Cu chromite in the presence of basic Mg-Al mixed oxides derived from hydrotalcite-type (HT) precursors (Carlini et al., 2004) or Cu/Mg/Al mixed oxide catalysts obtained from HT precursors (Carlini et al., 2005). These last systems resulted active and selective towards the Guerbet alcohol formation not only in liquid but also in gas phase at moderate temperature (280 °C), reaching selectivity around 80 mol % at complete propanol conversion. The use of HT-derived mixed oxides was also reported for ethanol condensation both in liquid and in gas phase. These mixed oxides were used as $MgAlO_x$ (Carvalho et al., 2012; Di Cosimo et al., 1998, 2000; León et al., 2011a) or as metal-promoted catalysts (Hosoglu et al., 2015; León et al., 2011b; Marcu et al., 2009, 2013). The addition of Cu metal component significantly increased the dehydrogenating activity to acetaldehyde reducing the amount of ethylene formed by dehydration at temperature > 300°C (Hosoglu et al., 2015). Marcu et al. (2009) studied the valorization of bioethanol over Cu/Mg/Al mixed oxides obtained from HT precursors by calcination at 550 °C. The catalytic tests were carried out in autoclave under autogenic pressure, in the temperature range of 200-250 °C. The conversion was always lower than 10 mol %, and an optimum yield to BuOH was ascertained for Cu content in the mixed oxides between 5 and 10 at. % . The same authors also studied the effect of different cations in Me/Mg/Al systems (Me = Pd, Ag, Mn, Fe, Cu, Sm or Yb) reporting good performances with the Pd-containing mixed oxide (Marcu et al., 2013). A strict correlation between the amount of basic sites of medium and high strength and the selectivity to butanol was evidenced, the presence of significant amount of acid sites increasing the selectivity to acetaldehyde and its acetal 1,1-diethoxyethane. The role of acid-base properties in the Guerbet condensation of the mixture of methanol and ethanol has been recently well-evidenced also for MgAl-HT derived oxides with different Mg/Al ratios (Li, X.N. et al., 2018; Stošić et al., 2017). The highest conversion was found for materials with the highest number of basic and acid sites. If the positive effect of basic sites was expected, the positive role of a certain acidity was related to the catalytic effect on aldol reaction and aldol dehydration. Recently

pre-reduced Ni/Mg/Al HT-derived mixed oxides were tested in flow reactor and EtOH conversion increased linearly from 7 to 22 % when the temperature was increased from 200 to 275 °C, the selectivity to BuOH remaining around 50 mol % (Pang et al., 2016). Interesting performances in the Guerbet condensation of ethanol were also ascertained in supercritical conditions at 310 °C and 80 atmospheres using Ni/Cu/Mg/Al HT-derived mixed oxides, although under these harsh reaction conditions the C-balance was only around 75 % due to the formation of volatile byproducts. On the other hand, when the same catalysts were adopted at 220 °C in the liquid phase, better C-balance but also much lower catalytic performances were ascertained (Sun et al., 2017). In summary, up to now heterogeneous systems able to afford good yields to BuOH working in liquid phase at temperatures lower than EtOH critical temperature have not been developed, due to the low activity and the prevailing or significant formation of different byproducts (in particular ethers and esters). In this work, Guerbet reaction was studied employing ad hoc synthesized Cu/Mg/Al HT-derived (Cu-HT) mixed oxides of different composition in order to establish relationships among the catalytic performances and their main physico-chemical and morphological properties.

## 2. Materials and Methods

### *2.1 Materials*

EtOH (Aldrich) was dried by distillation under dry argon after refluxing for 6 h on magnesium methoxide. Cu/Mg/Al HT precursors were prepared by coprecipitation at constant pH; a 2 M solution containing $Cu(NO_3)_2 \cdot 2.5H_2O$, $Mg(NO_3)_2 \cdot 6H_2O$ and $Al(NO_3)_3 \cdot 9H_2O$ in the appropriate ratios was slowly added to a 1 M solution containing $Na_2CO_3$ and NaOH. The atomic ratios percent (a.r.%) used in this work were: Cu/Mg/Al = 7.6/62.7/29.7, 2.8/68.2/29.0, and 1.0/69.0/30.0. The pH was kept constant (10.5 ± 0.2) by dropwise NaOH addition. The obtained precipitate was kept in suspension under stirring at 60 °C for 45 min, then filtered and washed with distilled water until a $Na_2O$ content lower than 0.02 wt.% was obtained. The precipitate was dried overnight at 60 °C and calcined at 500 °C for 7 h. The samples were labelled Cu7.6, Cu2.8 and Cu1.0, indicating the Cu a.r. A commercial Mg/Al hydrotalcite MG Puralox 79/390 was purchased by Sasol (MgO: 74.0 wt %, $Al_2O_3$: 26.0 wt %), calcined at 500 °C for 7 h and stored under dry argon.

### *2.2 Catalyst characterization*

The X-ray diffraction (XRD) analysis of the powders was carried out using a PANalytical X'Pert diffractometer equipped with a copper anode ($\lambda$mean = 0.15418 nm) and a fast X'Celerator detector. Wide-angle diffractogram was collected over 2$\theta$ range from 5 to 70° with a step size of 0.05° and counting time 15 s.

Specific surface area assessment was carried out using a Micromeritics ASAP 2020 instrument; samples were heated up to 150 °C and evacuated at a pressure better than 0.02 Torr, and kept for 150 min at this temperature.

Temperature programmed reduction by $H_2$ ($H_2$-TPR) was performed in an AutoChem II apparatus (Micromeritics) with pelletized catalysts. The catalyst was firstly cleaned at 150 °C under 30 mL/min He flow for 30 min. After cooling to 50 °C, the carrier gas was switched to 5 % $H_2$/Ar (v/v) at 30 mL/min. When the baseline was stable, the temperature was increased up to 800 °C with a heating rate of 10 °C/min, while the amount of $H_2$ consumed was measured by means of a thermal conductivity detector (TCD).

Temperature programmed desorption of $CO_2$ ($CO_2$-TPD) experiments were performed in an Autochem II (Micromeritics) instrument with powdered catalysts. The sample was placed in a quartz tubular reactor and pretreated at 500 °C under 30 mL/min He flow for 120 min, then cooled down to 40 °C and exposed to 10 % $CO_2$/He (v/v) stream with a flow rate of 30 mL/min for 2 h. The physisorbed $CO_2$ was removed by He purging (30 mL/min) for 60 min. Then, the sample was heated at 10 °C/min up to 800 °C and the desorbed $CO_2$ was monitored and recorded using an online Mass spectrometer (Cirrus 2, MKS instruments) which was calibrated by manual injections of pure $CO_2$ (m/z = 44) pulses.

A blank test flowing only Ar showed no $CO_2$ desorption in the 30-500 °C range investigated, while $H_2O$ and $CO_2$ evolved above 500 °C, namely at higher temperatures than that for calcination, indicating the not total dehydroxilation and decarbonation of the samples, thus the range analyzed for studying the basicity of the samples was 40-500 °C.

High resolution transmission electron microscopy (HRTEM) characterization was carried out by a TEM/STEM FEI TECNAI F20 microscope, equipped with an EDS analyzer. Powder catalysts were suspended in ethanol under ultrasounds for 20 min. The suspension was subsequently deposited on an Au grid with lacey multi-foil carbon film and dried at 100 °C before doing the measurement.

X-Ray Photoelectron Spectroscopy (XPS) data were collected using a Physical Electronics PHI 5700 spectrometer with non-monochromatic Mg-Kα radiation (300 W, 15 kV, 1253.6 eV) for the analysis of the core level signals of the studied elements and with a multichannel detector. Spectra of powdered samples were recorded with a constant pass energy value of 29.35 eV, using a 720 μm diameter analysis area. Under these conditions, the Au $4f_{7/2}$ line was recorded with 1.16 eV FWHM at a binding energy of 84.0 eV. The spectrometer energy scale was calibrated using Cu $2p_{3/2}$, Ag $3d_{5/2}$, and Au $4f_{7/2}$ photoelectron lines at 932.7, 368.3, and 84.0 eV, respectively. The Cu 2p and C 1s core level spectra were first recorded with a short irradiation time of 10 min to avoid, as much as possible, photoreduction of $Cu^{2+}$. The PHI ACCESS ESCA-V6.F software package was used for

acquisition and data analysis. The recorded spectra were always fitted using Gauss–Lorentz curves, in order to determine the binding energy of the different elements core levels more accurately.

The copper content of the employed catalysts Cu7.6, Cu2.8 and Cu1.0 was determined by Inductive Coupled Plasma Spectroscopy (ICPS) using a Jobin-Yvon JY 2000 Analizer. The samples were weighed into Teflon bombs followed by addition of acid mixture. Thereafter, microwave oven (MARS) was applied in the digestion and appropriate dilutions were performed prior to the ICP analysis. Microwave digestion was carried out in a CEM microwave accelerated reaction system MARS 6.

*2.3 Catalytic reactions*

The Guerbet condensation of EtOH was carried out in a batch reaction system, using a 300 ml Parr autoclave, with a mechanical stirrer and a heating system controlled by means of a Parr controller 4848. The proper amount of solid catalyst was introduced in the reactor under dry argon, then this was evacuated and 893 mmol of EtOH (52.12 ml) with 350 µl of benzene as internal standard were added through the sampling valve. When either MG Puralox was used as ancillary base or $MgSO_4$ was used as dehydrating component, they were introduced in the reactor successively to the copper catalyst, before the evacuation of the autoclave. The reactor was subsequently pressurized with $N_2$ (4 MPa) and heated at the programmed temperature (215-230 °C).

When the catalyst was beforehand pre-reduced, the proper amount of heterogeneous catalyst and 60 ml of MeOH were introduced in the reactor as described above, the autoclave was pressurized with $H_2$ up to 5 MPa and heated at 180 °C for 5 h for the metal component pre reduction. Then the reactor was evacuated, MeOH was removed under vacuum and then EtOH was introduced by suction. The reactor was subsequently pressurized with $N_2$ (4 MPa) and heated at the chosen temperature value (215 or 230 °C).

The reaction profile was followed by collecting at different times little portions of the reaction mixture through the sample valve and quickly cooling at 0 °C. At the end of each experiment the reactor was rapidly cooled at room temperature and slowly degassed. Finally, the liquid reaction mixture was analyzed by a GC-FID DANI GC1000 gas-cromatograph equipped with a HP PONA column (50 m x 0.2 mm x 0.5 µm) in order to determine EtOH conversion and product yields. The reaction products in the liquid phase were also identified by GC-MS, using a 6890N GC system gas chromatograph coupled with a 5975 mass selective detector single quadrupole mass spectrometer (Agilent Technologies).

The C-balance was always in the range 96-99 %, accounting for a loss of liquid during transfer after reaction, while the absence of ethylene in the gas phase was always ascertained by GC analysis.

The product molar yields (Y %), selectivity and ethanol conversion were calculated as:

$$Y\ (\%): \frac{\text{Moles of carbon in the target product}}{\text{Moles of carbon in fed ethanol}} \times 100$$

$$\text{Conv. } \%: \frac{\text{Moles of reacted ethanol}}{\text{Moles of fed ethanol}} \times 100$$

$$\text{Sel. } \%: \frac{\text{Moles of carbon in the target product}}{\text{Moles of carbon in reacted ethanol}} \times 100$$

Space time yield (STY) of product was calculated as STY = g product $kgcat^{-1}$ $h^{-1}$.

Leaching tests were carried out adopting the following procedure: at the end of the Guerbet reaction the solid catalyst was filtered off under inert atmosphere and the recovered liquid mixture was allowed to proceed for further 6h.

## Results and Discussion

*3.1 Synthesis and characterization of the catalysts*

The catalyst precursors showed the typical diffraction pattern of pristine HT-type compounds (Figure 1a) (Cavani et al., 1991), in agreement with the incorporation of the Jahn-Teller distorted $Cu^{2+}$ into the brucite-type sheets, favored by the presence of $Mg^{2+}$ (Kannan et al., 2004, 2005).

Figure 1, near here

The HT precursors were macroporous or non porous materials that agglomerated forming interparticle slit shaped pores, as revealed by their type IIb $N_2$ adsorption/ desorption isotherms (Rouquerol et al., 2014). The specific surface area values around 70-78 $m^2/g$ were not largely modified with the Cu loading, as evidenced in Table 1.

Table 1, near here

HRTEM images revealed that the samples were constituted by amorphous lamellar nanoparticles (60-70 nm) with rounded edges (Figure S1). EDS analysis confirmed that the composition of the precipitated solids was similar to the theoretical one.

The topotactic decomposition of the lamellar structure took place during calcination at 500 ºC for 7 h. A poorly crystallized MgO-type phase was developed (Figure 1b) wherein $Cu^{2+}$ and $Al^{3+}$ were included forming a mixed oxide (Chmielarz et al., 2003; Kannan et al., 2005; Montanari et al., 1997). The reflections were slightly more intense and narrow as the copper loading decreased. The presence of small CuO clusters in the high loading catalyst were not detectable by XRD, although

their presence could not be discarded (Bravo-Suárez et al., 2012; Montanari et al., 1997). Specific surface area values of calcined samples were around 132-143 $m^2/g$.

The incorporation of $Cu^{2+}$ species into the oxide structure was supported by $H_2$-TPR profiles, shown in Figure 2.

Figure 2, near here

$H_2$ consumption peaks were centred at higher temperatures in comparison to segregated CuO (Han et al., 2016). The onset and maximum of the reduction peaks shifted towards higher temperatures as the copper content decreased, due to better dispersed and stabilised copper species (Chmielarz et al., 2005; Montanari et al., 1997). The small peak at ca. 630 °C in Cu2.8 and Cu1.0 catalysts could be related to the formation of a copper spinel, e.g. $CuAl_2O_4$ (Alejandre et al., 1999).

The copper content determined by ICP analysis of the synthesized catalysts Cu7.6, Cu2.8 and Cu1.0 was found to be in very good agreement with the theoretically expected values, resulting 7.58, 2.79 and 1.01 as Cu a.r.% respectively, thus indicating very good incorporation of the metal ions into the hydrotalcite structures.

The basicity of the catalysts was evaluated by $CO_2$-TPD measurements, reported in Figure 3.

Figure 3, near here

The evolution of $CO_2$ occurred in the 50-500 °C range, characteristic of HT-derived catalysts containing basic sites of different strength (Bolognini et al., 2003; Di Cosimo et al., 1998). The amount of $CO_2$ desorbed decreased as the Cu content increased, as highlighted in Table 2.

Table 2, near here

The desorption profiles showed an asymmetric shape that can be deconvoluted into three peaks related to weak (around 105-110 °C), medium (135-145 °C) and strong (234-252 °C) basic sites, attributed to weakly basic Brønsted OH groups, M-O Lewis surface pairs and Lewis $O^{2-}$ groups. The three catalysts contained a larger amount of strong basic sites than low and medium sites, which decreased for higher Cu-loadings in the catalyst formulation.

*3.2 Catalytic conversion of ethanol*

The three calcined catalysts were compared in EtOH condensation carried out at 215 °C, adopting similar amounts of MgO basic component and a ratio MgO/EtOH in the range 0.066-0.076 mol/mol (Figure 4).

Figure 4, near here

Figure 4 reveals that this temperature is enough to reach interesting conversion levels for each tested system. At short reaction times (3-6 h) a progressive increase of the substrate conversion was observed moving from Cu7.6 to Cu1.0, i.e. decreasing the concentration of the Cu

hydrogenating/dehydrogenating component and increasing the number of basic sites, mainly the strong ones. In fact, Cu1.0 allowed at 215 °C, after 6 h a substrate conversion of 24.7 % with a selectivity in BuOH of 53 mol % (Figure 4a). The main by-products resulted higher alcohols (h.a.), mainly n-hexanol (selectivity = 21.6 mol %) and 1-octanol (selectivity = 10.2 mol %), while the selectivity in ethyl acetate (AcOEt) was as little as 2.4 mol %. The space-time yield (STY) of BuOH was 210, while the STY of the two higher linear alcohols (BuOH + HexOH) was 293. This result is excellent among the up to now reported heterogeneous catalysts when employed under similar and also higher temperatures (Marcu et al., 2013; Sun et al. 2017). The Cu content has an even more striking effect on the product distribution. In fact, when the Cu-rich Cu7.6 system was employed (Figure 4c) not only a lower EtOH conversion (18.1 mol %) was obtained, with a selectivity in BuOH of 56 mol %, but ethyl acetate resulted the main byproduct (selectivity = 27.4 mol %), HexOH selectivity being only 4.0 mol % after 6 h of reaction. Cu2.8 showed an intermediate behavior, in terms of activity and selectivity (Figure 4b). These results underline the relevant role of Cu content on the catalytic performances, previously reported for this reaction using much less active Cu-Mg-Al mixed oxide catalysts (Marcu et al., 2009). The loading determined the copper reducibility and basicity in the fresh catalysts, as previously commented, and possibly the copper particle size. In addition, in order to exclude Cu leaching from the employed systems, the liquid mixture recovered by filtration after 6h of reaction at 215°C in the presence of Cu7.6 was allowed to proceed for further 6h under the same reaction conditions and no further advancement of the reaction was ascertained, supposing the absence of Cu leaching. This result was additionally confirmed by ICP analysis of the final liquid mixture recovered after 12 h of reaction which excluded copper leaching, highlighting as the employed catalysts work in heterogeneous phase.

The characterization of the spent samples revealed, however, structural and morphological changes in the catalysts during reaction conditions altering the catalyst properties.

The structure and therefore the basicity of the samples were modified under the reaction conditions, as evidenced in Figure 5a.

Figure 5, near here

The HT layered structure was reconstructed (Figure 5a) due to the memory effect of the mixed oxides in presence of co-produced water, i.e. 1 mol $H_2O$ per mol BuOH (Sato et al., 1988). Anions, such as ethoxy and butoxy could be intercalated in the interlayer region adopting different configurations (Costantino et al., 1998; Gardner et al., 2001; Valente et al., 2007; Wang et al., 2014), in agreement with the shift of the basal reflections towards lower diffraction angles than in the original HT compound. As a result of the structural transformation, medium Mg-O and strong $O^{2-}$ Lewis basic sites in the calcined catalyst were removed in the hydrated sample (Debecker et al.,

2009; Di Cosimo et al., 1998; Marcu et al., 2009; Prinetto et al., 2000). On the other hand, the intercalated alkoxy or $OH^-$ anions were Brønsted basic sites. The former have been reported to catalyse the Guerbet condensation both in heterogeneous (Carlini et al., 2004) and homogeneous processes (Chakraborty et al., 2015). Besides, Mg/Al HT compounds intercalated with tert-butoxide were a strong heterogeneous base in transterification reactions (Choudary et al., 2000; Fu et al., 2017). On the other hand, $OH^-$ intercalated Mg/Al HT compounds are well-known catalysts in aldol condensation. Indeed, partially decomposed hydrotalcite-type compounds were used for Guerbet reaction (Tsuchida et al., 2001). However, for intercalated samples the accessibility of the reagents to the basic active sites should be considered, since only the anions near the edges of the HT platelet particles may be available (Abelló et al., 2005; Winter et al., 2006).

The activity seemed not to be directly related to the copper particle size, but mainly to Cu-content, which also controlled oxidation state and chemical environment. In both spent Cu7.6 and Cu1.0, spherical and ill-shaped Cu particles deposited over nanoparticles and large HT platelets (Figure 6a, 6b, 6f, 6g), with a large and broad size distribution (Figure 6e, 6i) were ascertained, probably because of the the coalescence of copper particles during reaction conditions, visible in Figure 6h. Moreover, some trigonal and hexagonal particles probably related to $Cu_2O$ were identified (Figure 6c, 6d).

Figure 6, near here

Copper was partially reduced to $Cu^0$, as revealed by XRD (Figure 5a) and XPS measurements summarized in Table 3 and Figures S2 and S3. In the spectra of Cu7.6, the main Cu2$p_{3/2}$ signal was composed of two contributions at 932.9 and 934.8 eV due to $Cu^0$ and $Cu^{2+}$ probably on the mixed oxide (Crivello et al., 2005; Moulder et al., 1992), which shifted towards lower values, 931.6 and 933.6 eV, in Cu1.0 spectra due to metallic copper and the spinel $CuAl_2O_4$, respectively, together with $Cu^{2+}$ in the mixed oxide. The ratio of the areas of the satellite region and the main signal ($I_{sat}/I_{mp}$) and the $Cu^0/Cu^{2+}$ ratio, which modified the hydrogenating/dehydrogenating activity, resulted metal loading dependent. The amount of $Cu^0$ species increased with the copper loading, thus, the Cu7.6 catalyst had a higher dehydrogenating activity favouring the formation of intermediate acetaldehyde, which then gives AcOEt by dehydrogenative route involving the hemiacetal (Inui et al., 2004).

A very interesting result was reached when the condensation was carried out using the same catalysts after a pre-reduction step at 180 °C in methanol under 5 MPa of $H_2$, as shown in Figure 7.

Figure 7, near here

In the case of Cu7.6 the pre-reduction caused a low decrease of the activity and a significant drop of the selectivity in BuOH (from 56.6 to 37.7 after 6h, with a corresponding increase of that in AcOEt

from 27.4 to 53.4 mol. %). On the other hand, a positive effect of the prereduction was ascertained for Cu2.8 and Cu1.0. When pre-reduced Cu1.0 was tested, after 6 h at 215 °C EtOH conversion reached 29.8 %, with a selectivity in BuOH of 57.4 mol % (corresponding to a STY of BuOH of 270). The pre-reduction modified the copper particle size (Figure 8) rather than the oxidation state (Table 3 and Figures S2 and S3) in the spent catalysts and consequently their activity in dehydrogenation/hydrogenation steps.

Figure 8, near here

The pretreatment reduced the sintering, an effect more remarkable at low Cu-loading, i.e. the copper particle sizes in Cu7.6 were in the 10-60 nm range (Figure 8a, 8d), while Cu1.0 contained well dispersed 1 to 10 nm particles (Figure 8e, 8g), together with particles up to 135 nm (Figure 8f, 8h). The decrease in the particle size in both catalysts could enhance the activities previously commented, namely the formation of the esters for the high Cu-loaded catalyst and the BuOH production for the low Cu-loaded one. The spent Cu7.6 catalyst, which produced lower BuOH, generated less water and was less rehydrated than Cu2.8 and Cu1.0 (Figure 5b); this may also contribute to the preservation of some properties of the catalyst after reduction (Figures S4 and S5), although the sintering by coalescence also happened (Figure 8b, 8c).

The best catalytic system Cu1.0 was also tested at 230°C and the results are reported in Table 4.

Table 4, near here

The temperature increase caused an increase of the activity, mainly at short reaction time: after 3 h at 230 °C the space-time yield (STY) of BuOH reached 372, a remarkable result up to now never reported to date in the literature for this reaction performed under similar conditions.

In order to confirm the importance of a low Cu content to achieve high yields in higher alcohols and reduce the amount of formed ester, the effect of the progressive reduction of the copper-rich Cu7.6 amount was studied, compensating for the low amount of Mg/Al mixed oxide species by adding those derived from a commercial HT compound (MG Puralox). The obtained results reported in Figure 9 perfectly confirm that the lowering of the introduced Cu amount, if the depletion of Mg/Al component is counterbalanced, leads to complete turn of the catalytic behavior.

Figure 9, near here

In fact, moving from the pure Cu7.6 catalyst (Figure 9a) to decreasing Cu7.6 amounts (Figure 9b, 9c), a progressive increase of the conversion and, above all, a marked enhancement of the selectivity in higher alcohols was observed at expense of the AcOEt formation. When 1 mmol of Cu was employed (run c in Figure 9) the results were quite similar to those obtained in run a of Figure 4 where the catalyst Cu1.0 with the lowest loading was adopted, i.e. using the same amount of Cu. In fact, in this case after 6 h a conversion of 22 % of the EtOH was reached with selectivity in

butanol of 58.1 mol %. Also in this case the main byproduct turned to n-hexanol (selectivity = 18.2 mol%), while the selectivity in AcOEt dropped to 4.3 mol %. After 6 h the STY considering the introduced Cu7.6 system resulted 705, the highest value up to now reported using Cu-based systems.

On the other hand, when the pure commercial Mg/Al system was employed (Figure 9d) the activity was very low (EtOH conversion = 3.6 mol % after 6 h) but the selectivity to BuOH reached 67 mol %. These results underline the importance of the copper component, although in low concentration, in the mixed oxide and confirm the best performances ascertained for the Cu1.0 system, having lower metal loading.

For all the catalysts tested at 215 °C a decrease of the catalytic performances was observed as the reaction continued (Figure 4), due to water accumulated in the batch reactor which caused the reconstruction of the HT-type structure with the intercalation in the interlayer region of both $OH^-$ and large anions, probably alkoxy species (Figure 5). The reconstruction modified the copper particle size and the type and accessibility of the basic sites.

Therefore, the effect of water removal was studied, by addition of anhydrous $MgSO_4$, as reported in Figure 10.

Figure 10, near here

As previously observed by Marcu et al. (2009), the addition of the drying agent enhanced the catalytic activity: the EtOH conversion after 12 h moved from 28.2 % to 34.7 % and also the selectivity in BuOH was slightly increased. These positive effects of the water removal could be related to the preservation of Lewis stronger basic sites $O^{2-}$ rather than their transformation into weaker Brønsted $OH^-$ ones. In the case of higher linear $C_8$, $C_{10}$ and $C_{18}$ alcohols Guerbet condensation in the presence of Ni/Cu hydrotalcite derived mixed oxides high catalytic stability is ascertained when water is continuously removed using a with a Dean–Stark azeotrope trap (Hernandez et al., 2016).

## Conclusions

The tailoring in the Cu-content in hydrotalcite-derived Cu/Mg/Al mixed oxides allowed us to obtain good performances in the Guerbet condensation of ethanol to butanol carried out in the liquid phase at 215-230 °C. A low Cu-content was required to decrease the ester formation and favour the aldol condensation to butanol and higher alcohols. The differences in the activity and selectivity were related to the metallic/acid/basic sites in the fresh catalysts, a decrease in the copper content increasing the basic sites and decreasing Cu reducibility. Besides, the original HT structure was partially reconstructed under reaction conditions due to the water co-produced, $Cu^{2+}$ partially

reduced and copper particles sintered, therefore modifying the type and accessibility of basic and metallic sites. The catalyst Cu1.0 with the lowest Cu loading contained a lower $Cu^0/Cu^{2+}$ ratio after catalytic tests than a high loaded one, but rather similar copper particle sizes due to the coalescence; providing less hydrogenation sites and decreasing the ester formation. A pre-reduction treatment delayed the sintering and enhanced the activities in alcohol and ester formation for low and high loaded catalysts, respectively. These promising performances can be enhanced by removing the co-produced water which caused the reconstruction of the HT structure by adding a drying agent, while the study of this reaction in flow reactor is now in progress.

## References


Abelló, S., Medina, F., Tichit, D., Pérez-Ramírez, J., Groen, J.C., Sueiras, J.E., Salagre, P., Cesteros, Y., 2005. Aldol condensations over reconstructed Mg-Al hydrotalcites: Structure-activity relationships related to the rehydration method. Chem. Eur. J. 11, 728–739. https://doi.org/10.1002/chem.200400409.

Alejandre, A., Medina, F., Salagre, P., Correig, X., Sueiras, J.E., 1999. Preparation and study of Cu-Al mixed oxides via hydrotalcite-like precursors. Chem. Mater. 11, 939–948. https://doi.org/10.1021/cm980500f.

Bolognini, M., Cavani, F., Scagliarini, D., Flego, C., Perego, C., Saba, M., 2003. Mg/Al mixed oxides prepared by coprecipitation and sol-gel routes: a comparison of their physico-chemical features and performances in *m*-cresol methylation. Microporous Mesoporous Mater. 66, 77–89. https://doi.org/10.1016/j.micromeso.2003.09.010.

Bravo-Suárez, J.J., Subramaniam, B., Chaudhari, R.V., 2012. Ultraviolet-visible spectroscopy and temperature-programmed techniques as tools for structural characterization of Cu in $CuMgAlO_x$ mixed metal oxides. J. Phys. Chem. C 116, 18207–18221. https://doi.org/10.1021/jp303631v.

Britto Júnior, R.F., Martins, C.A., 2015. Emission analysis of a diesel engine operating in diesel-ethanol dual-fuel mode. Fuel 148, 191–201. https://doi.org/10.1016/j.fuel.2015.01.008.

Carlini, C., Di Girolamo, M., Macinai, A., Marchionna, M., Noviello, M., Raspolli Galletti, A.M., Sbrana, G., 2003a. Selective synthesis of isobutanol by means of the Guerbet reaction: Part 2. Reaction of methanol/ethanol and methanol/ethanol/*n*-propanol mixtures over copper based/MeONa catalytic systems. J. Mol. Catal. A 200, 137–146. https://doi.org/10.1016/S1381-1169(03)00042-6.

Carlini, C., Di Girolamo, M., Macinai, A., Marchionna, M., Noviello, M., Raspolli Galletti, A.M., Sbrana, G., 2003b. Synthesis of isobutanol by the Guerbet condensation of methanol with *n*-

propanol in the presence of heterogeneous and homogeneous palladium-based catalytic systems. J. Mol. Catal. A 204-205, 721–728. https://doi.org/10.1016/S1381-1169(03)00357-1.

Carlini, C., Flego, C., Marchionna, M., Noviello, M., Raspolli Galletti, A.M., Sbrana, G., Basile, F., Vaccari, A., 2004. Guerbet condensation of methanol with *n*-propanol to isobutyl alcohol over heterogeneous copper chromite/Mg-Al mixed oxides catalysts. J. Mol. Catal. A 220, 215–220. https://doi.org/10.1016/j.molcata.2004.05.034.

Carlini, C., Macinai, A., Marchionna, M., Noviello, M., Raspolli Galletti, A.M., Sbrana, G., 2003c. Selective synthesis of isobutanol by means of the Guerbet reaction: Part 3: Methanol/*n*-propanol condensation by using bifunctional catalytic systems based on nickel, rhodium and ruthenium species with basic components. J. Mol. Catal. A 206, 409–418. https://doi.org/10.1016/S1381-1169(03)00453-9.

Carlini, C., Di Girolamo, M., Marchionna, M., Noviello, M., Raspolli Galletti, A.M., Sbrana, G., 2002. Selective synthesis of isobutanol by means of the Guerbet reaction: Part 1. Methanol/*n*-propanol condensation by using copper based catalytic systems. J. Mol. Catal. A 184, 273–280. https://doi.org/10.1016/S1381-1169(02)00007-9.

Carlini, C., Marchionna, M., Noviello, M., Raspolli Galletti, A.M., Sbrana, G., Basile, F., Vaccari, A., 2005. Guerbet condensation of methanol with *n*-propanol to isobutyl alcohol over heterogeneous bifunctional catalysts based on Mg-Al mixed oxides partially substituted by different metal components. J. Mol. Catal. A 232, 13–20. https://doi.org/10.1016/j.molcata.2004.12.037.

Carvalho, D.L., de Avillez, R.R., Rodrigues, M.T., Borges, L.E.P., Appel, L.G., 2012. Mg and Al mixed oxides and the synthesis of *n*-butanol from ethanol. Appl. Catal. A: Gen. 415–416, 96–100. https://doi.org/10.1016/j.apcata.2011.12.009.

Cavani, F., Trifiró, F., Vaccari, A., 1991. Hydrotalcite-type anionic clays: Preparation, properties and applications. Catal. Today 11, 173–301. https://doi.org/10.1016/0920-5861(91)80068-K.

Chakraborty, S., Piszel, P.E., Hayes, C.E., Baker, R.T., Jones, W.D., 2015. Highly selective formation of *n*-butanol from ethanol through the Guerbet process: A tandem catalytic approach. J. Am. Chem. Soc. 137, 14264–14267. https://doi.org/10.1021/jacs.5b10257.

Chieregato, A., Velasquez Ochoa, J., Bandinelli, C., Fornasari, G., Cavani, F., Mella, M., 2015. On the chemistry of ethanol on basic oxides: Revising mechanisms and intermediates in the Lebedev and Guerbet reactions. ChemSusChem 8, 377–388. https://doi.org/10.1002/cssc.201402632.

Chmielarz, L., Kuśtrowski, P., Rafalska-Łasocha, A., Dziembaj, R., 2003. Influence of Cu, Co and Ni cations incorporated in brucite-type layers on thermal behaviour of hydrotalcites and

reducibility of the derived mixed oxide systems. Thermochim. Acta 395, 225–236. https://doi.org/10.1016/S0040-6031(02)00214-9.

Chmielarz, L., Kuśtrowski, P., Rafalska-Łasocha, A., Dziembaj, R., 2005. Selective oxidation of ammonia to nitrogen on transition metal containing mixed metal oxides. Appl. Catal. B: Environ. 58, 235–244. https://doi.org/10.1016/j.apcatb.2004.12.009.

Choudary, B.M., Kantam, M.L., Reddy, C.V., Aranganathan, S., Santhi, P.L., Figueras, F., 2000. Mg-Al-O-*t*-Bu hydrotalcite: A new and efficient heterogeneous catalyst for *trans*esterification. J. Mol. Catal. A 159, 411–416. https://doi.org/10.1016/S1381-1169(00)00209-0.

Costantino, U., Marmottini, F., Nocchetti, M., Vivani, R., 1998. New synthetic routes to hydrotalcite-like compounds-Characterisation and properties of the obtained materials. Eur. J. Inorg. Chem. 1998, 1439–1446. https://doi.org/10.1002/(SICI)1099-0682(199810)1998:10<1439::AID-EJIC1439>3.0.CO;2-1.

Crivello, M., Pérez, C., Herrero, E., Ghione, G., Casuscelli, S., Rodriguez-Castellón, E., 2005. Characterization of Al-Cu and Al-Cu-Mg mixed oxides and their catalytic activity in dehydrogenation of 2-octanol. Catal. Today 107–108, 215–222. https://doi.org/10.1016/j.cattod.2005.07.168.

Debecker, D.P., Gaigneaux, E.M., Busca, G., 2009. Exploring, tuning, and exploiting the basicity of hydrotalcites for applications in heterogeneous catalysis. Chem. Eur. J. 15, 3920–3935. https://doi.org/10.1002/chem.200900060.

Di Cosimo, J.I., Apesteguía, C.R., Ginés, M.J.L., Iglesia, E., 2000. Structural requirements and reaction pathways in condensation reactions of alcohols on $Mg_yAlO_x$ catalysts. J. Catal. 190, 261–275. https://doi.org/10.1006/jcat.1999.2734.

Di Cosimo, J.I., Díez, V.K., Xu, M., Iglesia, E., Apesteguía, C.R., 1998. Structure and surface and catalytic properties of Mg-Al basic oxides. J. Catal. 178, 499–510. https://doi.org/10.1006/jcat.1998.2161.

Dowson, G.M.R., Haddow, M.F., Lee, J., Wingad, R.L., Wass, D.F., 2013. Catalytic conversion of ethanol into an advanced biofuel: Unprecedented selectivity for n-butanol. Angew. Chem. Int. Ed. 52, 9005–9008. https://doi.org/10.1002/anie.201303723.

Fu, S., Shao, Z., Wang, Y., Liu, Q., 2017. Manganese-catalyzed upgrading of ethanol into 1-butanol. J. Am. Chem. Soc. 139, 11941–11948. https://doi.org/10.1021/jacs.7b05939.

Gabriëls, D., Hernández, W.Y., Sels, B., Van Der Voort, P., Veberckmoes, A., 2015. Review of catalytic systems and thermodynamics for the Guerbet condensation reaction and challenges

for biomass valorization. Catal. Sci. Technol. 5, 3876–3902. https://doi.org/10.1039/C5CY00359H.

Gardner, E., Huntoon, K.M., Pinnavaia, T.J., 2001. Direct synthesis of alkoxide-intercalated derivatives of hydrotalcite-like layered double hydroxides: Precursors for the formation of colloidal layered double hydroxide suspensions and transparent thin films. Adv. Mater. 13, 1263–1266. https://doi.org/10.1002/1521-4095(200108)13:163.0.CO;2-R.

Han, J., Zeng, H.-Y., Xu, S., Chen, C.-R., Liu, X.-J., 2016. Catalytic properties of CuMgAlO catalyst and degradation mechanism in CWPO of methyl orange. Appl. Catal. A: Gen. 527, 72–80. https://doi.org/10.1016/j.apcata.2016.08.015.

Hernández, W.Y., De Vlieger, K., Van Der Voort, P., Verberckmoes, A., 2016 Ni−Cu Hydrotalcite-Derived Mixed Oxides as Highly Selective and Stable Catalysts for the Synthesis of β-Branched Bioalcohols by the Guerbet Reaction. ChemSusChem, 9 (22), 3196-3205. https://doi.org/10.1002/cssc.201601042.

Hosoglu, F., Faye, J., Mareseanu, K., Tesquet, G., Miquel, P., Capron, M., Gardoll, O., Lamonier, J.-F., Lamonier, C., Dumeignil, F., 2015. High resolution NMR unraveling Cu substitution of Mg in hydrotalcites-ethanol reactivity. Appl. Catal. A: Gen. 504, 533–541. https://doi.org/10.1016/j.apcata.2014.10.005.

Inui, K., Kurabayashi, T., Sato, S., Ichikawa, N., 2004. Effective formation of ethyl acetate from ethanol over Cu-Zn-Zr-Al-O catalyst. J. Mol. Catal. A 216, 147–156. https://doi.org/10.1016/j.molcata.2004.02.017.

Kannan, S., Dubey, A., Knözinger, H., 2005. Synthesis and characterization of CuMgAl ternary hydrotalcites as catalysts for the hydroxylation of phenol. J. Catal. 231, 381–392. https://doi.org/10.1016/j.jcat.2005.01.032.

Kannan, S., Rives, V., Knözinger, H., 2004. High-temperature transformations of Cu-rich hydrotalcites. J. Solid State Chem. 177, 319–331. https://doi.org/10.1016/j.jssc.2003.08.023.

Kozlowski, J.T., Davis, R.J., 2013. Heterogeneous catalysts for the Guerbet coupling of alcohols. ACS Catal. 3, 1588–1600. https://doi.org/10.1021/cs400292f.

León, M., Díaz, E., Ordóñez, S., 2011a. Ethanol catalytic condensation over Mg-Al mixed oxides derived from hydrotalcites. Catal. Today 164, 436–442. https://doi.org/10.1016/j.cattod.2010.10.003.

León, M., Díaz, E., Vega, A., Ordóñez, S., Auroux, A., 2011b. Consequences of the iron-aluminium exchange on the performance of hydrotalcite-derived mixed oxides for ethanol condensation. Appl. Catal. B: Environ. 102, 590–599. https://doi.org/10.1016/j.apcatb.2010.12.044.

Li, H., Riisager, A., Saravanamurugan, S., Pandey, A., Sangwan, R.S., Yang, S., Luque, R., 2018. Carbon-increasing catalytic strategies for upgrading biomass into energy-intensive fuels and chemicals. ACS Catal. 8, 148–187. https://doi.org/10.1021/acscatal.7b02577.

Li, X.N., Peng, S.S., Feng, L.N., Lu, S.Q., Ma, L.J., Yue, M.B., 2018. One-pot synthesis of acidic and basic bifunctional catalysts to promote the conversion of ethanol to 1-butanol. Microporous Mesoporous Mater. 261, 44–50. https://doi.org/10.1016/j.micromeso.2017.11.004.

Marcu, I.-C., Tanchoux, N., Fajula, F., Tichit, D., 2013. Catalytic conversion of ethanol into butanol over M-Mg-Al mixed oxide catalysts (M = Pd, Ag, Mn, Fe, Cu, Sm, Yb) obtained from LDH precursors. Catal. Lett. 143, 23–30. https://doi.org/10.1007/s10562-012-0935-9.

Marcu, I.-C., Tichit, D., Fajula, F., Tanchoux, N., 2009. Catalytic valorization of bioethanol over Cu-Mg-Al mixed oxide catalysts. Catal. Today 147, 231–238. https://doi.org/10.1016/j.cattod.2009.04.004.

Meunier, F.C., Scalbert, J., Thibault-Starzyk, F., 2015. Unraveling the mechanism of catalytic reactions through combined kinetic and thermodynamic analyses: Application to the condensation of ethanol. C.R. Chim. 18, 345–350. https://doi.org/10.1016/j.crci.2014.07.002.

Montanari, B., Vaccari, A., Gazzano, M., Käßner, P., Papp, H., Pasel, J., Dziembaj, R., Makowski, W., Lojewski, T., 1997. Characterization and activity of novel copper-containing catalysts for selective catalytic reduction of NO with $NH_3$. Appl. Catal. B: Environ. 13, 205–217. https://doi.org/10.1016/S0926-3373(96)00106-3.

Moulder, J.F., Stickle, W.F., Sobol, P.E., Bomben, K.D., 1992. Handbook of X-Ray photoelectron spectroscopy, Perkin-Elmer Corporation, Eden Prairie, United States of America.

Pang, J., Zheng, M., He, L., Li, L., Pan, X., Wang, A., Wang, X., Zhang, T., 2016. Upgrading ethanol to *n*-butanol over highly dispersed Ni-MgAlO catalysts. J. Catal. 344, 184–193. https://doi.org/10.1016/j.jcat.2016.08.024.

Pereira, L.G., Dias, M.O.S., Mariano, A.P., Filho, R.M., Bonomi, A., 2015. Economic and environmental assessment of *n*-butanol production in an integrated first and second generation sugarcane biorefinery: Fermentative versus catalytic routes. Appl. Energy 160, 120–131. https://doi.org/10.1016/j.apenergy.2015.09.063.

Prinetto, F., Ghiotti, G., Durand, R., Tichit, D., 2000. Investigation of acid-base properties of catalysts obtained from layered double hydroxides. J. Phys. Chem. B 104, 11117–11126. https://doi.org/10.1021/jp002715u.

Riittonen, T., Salmi, T., Mikkola, J.-P., Wärnå, J., 2014. Direct synthesis of 1-butanol from ethanol in a plug flow reactor: Reactor and reaction kinetics modeling. Top. Catal. 57, 1425–1429. https://doi.org/10.1007/s11244-014-0314-4.

Riittonen, T., Toukoniitty, E., Madnani, D.K., Leino, A.-R., Kordas, K., Szabo, M., Sapi, A., Arve, K., Wärnå, J., Mikkola, J.-P., 2012. One-pot liquid-phase catalytic conversion of ethanol to 1-butanol over aluminium oxide-The effect of the active metal on the selectivity. Catalysts 2, 68–84. https://doi.org/10.3390/catal2010068.

Rouquerol, F., Rouquerol, J., Sing, K.S.W., Llewellyn, P., Maurin, G., 2014. Adsorption by powders and porous solids. Principles, methodology and applications, second ed. Academic Press, Oxford.

Sato, T., Fujita, H., Endo, T., Shimada, M., Tsunashima, A., 1988. Synthesis of hydrotalcite-like compounds and their physico-chemical properties. React. Solids 5, 219–228. https://doi.org/10.1016/0168-7336(88)80089-5.

Singh, S.B., Dhar, A., Agarwal, A.K., 2015. Technical feasibility study of butanol-gasoline blends for powering medium-duty transportation spark ignition engine. Renew. Energ. 76, 706–716. https://doi.org/10.1016/j.renene.2014.11.095.

Sreekumar, S., Baer, Z.C., Gross, E., Padmanaban, S., Goulas, K., Gunbas, G., Alayoglu, S., Blanch, H.W., Clark, D.S., Toste, F.D., 2014. Chemocatalytic upgrading of tailored fermentation products toward biodiesel. ChemSusChem 7, 2445–2448. https://doi.org/10.1002/cssc.201402244.

Stošić, D., Hosoglu, F., Bennici, S., Travert, A., Capron, M., Dumeignil, F., Couturier, J.-L., Dubois, J.-L., Auroux, A., 2017. Methanol and ethanol reactivity in the presence of hydrotalcites with Mg/Al ratios varying from 2 to 7. Catal. Commun. 89, 14–18. https://doi.org/10.1016/j.catcom.2016.10.013.

Sun, Z., Vasconcelos, A.C., Bottari, G., Stuart, M.C.A., Bonura, G., Cannilla, C., Frusteri, F., Barta, K., 2017. Efficient catalytic conversion of ethanol to 1-butanol via the Guerbet reaction over copper- and nickel-doped porous. ACS Sustainable Chem. Eng. 5, 1738–1746. https://doi.org/10.1021/acssuschemeng.6b02494.

Tsuchida, T., Atsumi, K., Sakuma, S., Inui, T., 2001. Synthesis method of chemical industrial raw material and high-octane fuel, and high-octane fuel composition. Patent US 6,323,383 B1.

Valente, J.S., Cantú, M.S., Cortez, J.G.H., Montiel, R., Bokhimi, X., López-Salinas, E., 2007. Preparation and characterization of sol-gel MgAl hydrotalcites with nanocapsular morphology. J. Phys. Chem. C 111, 642–651. https://doi.org/10.1021/jp065283h.

Wang, H., Duan, W., Wu, Y., Tang, Y., Li, L., 2014. Synthesis of magnesium-aluminum layered double hydroxide intercalated with ethylene glycol by the aid of alkoxides. Inorg. Chim. Acta 418, 163–170. https://doi.org/10.1016/j.ica.2014.04.031.

Winter, F., Xia, X., Hereijgers, B.P.C., Bitter, J.H., van Dillen, A.J., Muhler, M., de Jong, K.P., 2006. On the nature and accessibility of the Brønsted-base sites in activated hydrotalcite catalysts. J. Phys. Chem. B 110, 9211–9218. https://doi.org/10.1021/jp0570871.

Wu, X., Fang, G., Tong, Y., Jiang, D., Liang, Z., Leng, W., Liu, L., Tu, P., Wang, H., Ni, J., Li, X. , 2018. Catalytic Upgrading of Ethanol to n-Butanol: Progress in Catalyst Development ChemSusChem, 11 (1), 71-85. https://doi.org/10.1002/cssc.201701590.

Zaccheria, F., Scotti, N., Ravasio, N., 2018. The role of copper in the upgrading of bioalcohols. ChemCatChem 10, 1526–1535. https://doi.org/10.1002/cctc.201701844.

Zhang, Q., Dong, J., Liu, Y., Wang, Y., Cao, Y., 2016. Towards a green bulk-scale biobutanol from bioethanol upgrading. J. Energy Chem. 25, 907–910. https://doi.org/10.1016/j.jechem.2016.08.010.

## Captions for Figures and for Scheme

**Figure 1:** a) Diffraction patterns of the catalyst precursors Cu7.6 HT, Cu2.8 HT and Cu1.0 HT; b) Diffraction patterns of the catalysts after calcination at 500 ºC for 7 h.

**Figure 2:** $H_2$-TPR profiles for the catalysts Cu7.6, Cu2.8 and Cu1.0.

**Figure 3:** $CO_2$-TPD profiles for the catalysts Cu7.6, Cu2.8 and Cu1.0.

**Figure 4:** Influence of Cu loading on the catalytic performances of the different catalysts at temperature 215 °C, EtOH 893 mmol: a) Cu1.0 catalyst, Cu: 1 mmol (MgO 67,9 mmol); b) Cu2.8 catalyst, Cu: 2.68 mmol (MgO 65,9 mmol); c) Cu7.6 catalyst, Cu: 7.1 mmol, (MgO 59 mmol). Other products: 2-ethyl-1-hexanol, 1,1-diethoxy-ethane, ethyl butyrate, 2-ethyl-1-butanol, 1-octanol.

**Figure 5:** a) Diffraction patterns of the spent catalysts Cu7.6, Cu2.8 and Cu1.0 and diffraction pattern of the catalyst precursor Cu1.0 HT; b) Diffraction patterns of the spent pre-reduced catalysts Cu7.6, Cu2.8 and Cu1.0, together with the diffraction pattern of the catalyst precursor Cu1.0 HT.

**Figure 6:** HRTEM characterization of Cu7.6 and Cu1.0 spent catalysts: HAADF/STEM images (a: Cu7.6; f: Cu1.0), HRTEM images (b, c, d: Cu7.6; g, h: Cu1.0) and particle size distributions (e: Cu7.6; i: Cu1.0).

**Figure 7:** Influence of the pre-reduction step on the catalytic performances of the different catalytic systems in EtOH condensation at 215 °C, EtOH 893 mmol: a) Cu7.6 catalyst, Cu: 7.1 mmol (MgO: 59 mmol); b) Cu2.8 catalyst, Cu: 2.7 mmol (MgO: 63.4 mmol); c) Cu1.0 catalyst, Cu: 1 mmol (MgO: 68.3 mmol). Other products: 2-ethyl-1-hexanol, 1,1-diethoxy-ethane, ethyl butyrate, 2-ethyl-1-butanol, 1-octanol.

**Figure 8:** HRTEM characterization of Cu7.6 and Cu1.0 pre-reduced spent catalysts: HRTEM images (a, b, c: Cu7.6; f: Cu1.0), HAADF/STEM image (e: Cu1.0), and particle size distributions (d: Cu7.6; g, h: Cu1.0).

**Figure 9:** Influence of the addition of commercial MG Puralox on the catalytic performances of Cu7.6 catalyst at 215 °C, EtOH 893 mmol: a) Cu7.6 catalyst, Cu: 7.1 mmol (MgO 59 mmol), MG Puralox: absent; b) Cu7.6 catalyst, Cu: 3.8 mmol (MgO 31,6 mmol) MG Puralox: 34.2 mmol of MgO; c) Cu7.6 catalyst, Cu: 1 mmol (MgO 8.3 mmol) MG Puralox: 63 mmol of MgO; d) Cu7.6: absent; MG Puralox: 73.1 mmol of MgO. Other products: 2-ethyl-1-hexanol, 1,1-diethoxy-ethane, ethyl butyrate, 2-ethyl-1-butanol, 1-octanol.

**Figure 10:** Influence of the presence of $MgSO_4$ on the catalytic performances of Cu7.6 at 215 °C, EtOH 893 mmol: a) Cu7.6 catalyst, Cu: 1 mmol, MgO 8.3 mmol, MG Puralox: 63 mmol of MgO; b) Cu7.6 catalyst, Cu: 1 mmol; MgO 8.3 mmol, MG Puralox: 63 mmol of MgO; $MgSO_4$: 3 g. Other products: 2-ethyl-1-hexanol, 1,1-diethoxy-ethane, ethyl butyrate, 2-ethyl-1-butanol, 1-octanol.

**Scheme 1:** Reaction network for Guerbet reaction.

**Table 1.** Specific surface area values of the HT precursors, fresh and spent catalysts

| Sample | $S_{BET}$ ($m^2/g$) | | | |
|---|---|---|---|---|
| | **HT** | **c500**[a] | **Spent** | **Spent prereduced** |
| Cu7.6 | 71 | 133 | 167 | 180 |
| Cu2.8 | 75 | 132 | 157 | 175 |
| Cu1.0 | 78 | 143 | 157 | 170 |

[a] samples after calcinations at 500°C for 7 h

**Table 2.** Basicity distribution of the catalysts from $CO_2$-TPD measurements

| Sample | µmol $CO_2$ / gcat | Low | Medium | Strong |
|---|---|---|---|---|
| Cu7.6 | 215 | 10 % | 15 % | 75 % |
| Cu2.8 | 276 | 12 % | 16 % | 72 % |
| Cu1.0 | 358 | 7 % | 11 % | 82 % |

**Table 3.** Binding energies of the Cu2p$_{3/2}$ peaks, values of Isat/Imp and $Cu^0/Cu^{2+}$ ratio for the Cu7.6 and Cu1.0 pre-reduced and not pre-reduced spent catalysts

| Sample | Prereduction | Peak | Position (eV) | Isat/Imp | $Cu^0/Cu^{2+}$ |
|---|---|---|---|---|---|
| Cu7.6 | No | Cu 2$p_{3/2}$ | 932.9<br>934.8 | 0.11 | 2.23 |
| Cu7.6 | Yes | | 932.8<br>934.8 | 0.20 | 1.78 |
| Cu1.0 | No | | 931.6<br>933.6 | 0.35 | 0.39 |
| Cu1.0 | Yes | | 931.9<br>933.5 | 0.40 | 0.32 |

**Table 4.** Effect of the temperature on EtOH condensation in the presence of Cu1.0 catalyst. Reaction conditions: EtOH 893 mmol, Cu: 1 mmol (MgO 67.9 mmol)

| Temperature (°C) | Time (h) | Conv. (mol %) | Selectivity (mol %) | | | | |
|---|---|---|---|---|---|---|---|
| | | | BuOH | AcOEt | HexOH | 2-EH | Others |
| 215 | 3 | 15.8 | 56.0 | 3.1 | 20.0 | 1.6 | 19.3 |
| | 6 | 24.7 | 53.0 | 2.4 | 21.6 | 2.1 | 20.6 |
| | 12 | 27.8 | 52.8 | 2.5 | 21.7 | 2.3 | 20.7 |
| 230 | 3 | 21.0 | 55.8 | 3.5 | 26.2 | 2.3 | 12.2 |
| | 6 | 26.1 | 57.5 | 3.4 | 18.9 | 1.9 | 18.3 |
| | 12 | 32.4 | 52.1 | 3.3 | 19.9 | 2.9 | 21.4 |

**Figure 1**

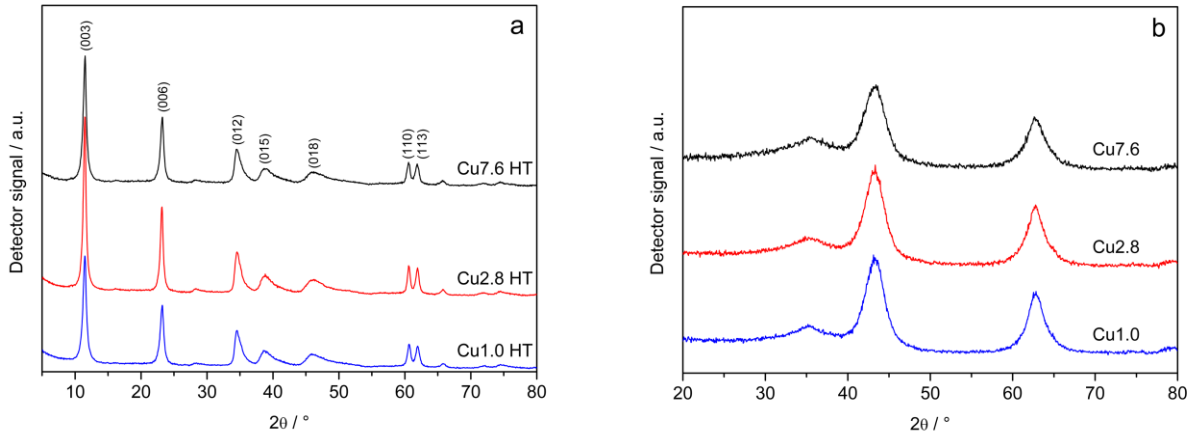


**Figure 1:** a) Diffraction patterns of the catalyst precursors Cu7.6 HT, Cu2.8 HT and Cu1.0 HT; b) Diffraction patterns of the catalysts after calcination at 500 ºC for 7 h.

**Figure 2**

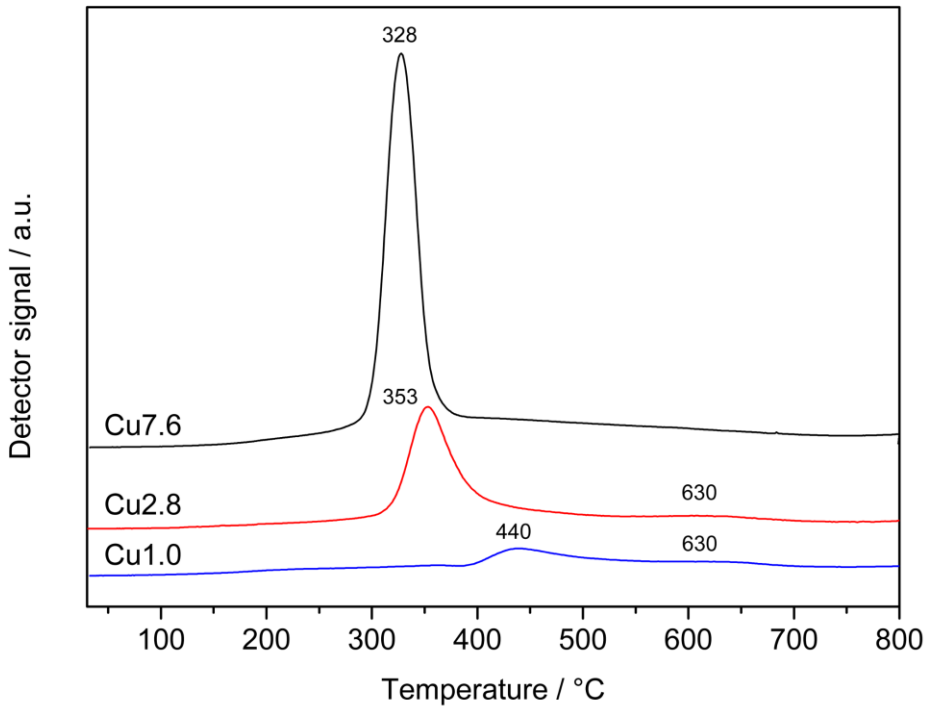


**Figure 2:** $H_2$-TPR profiles for the catalysts Cu7.6, Cu2.8 and Cu1.0.

**Figure 3**

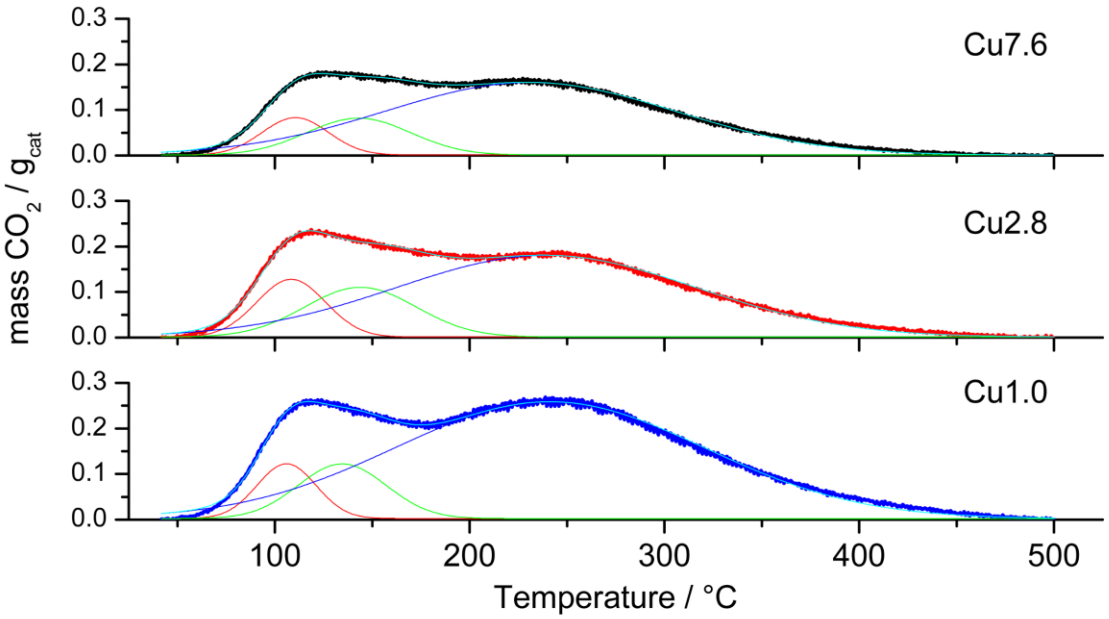


**Figure 3:** $CO_2$-TPD profiles for the catalysts Cu7.6, Cu2.8 and Cu1.0.

**Figure 4**

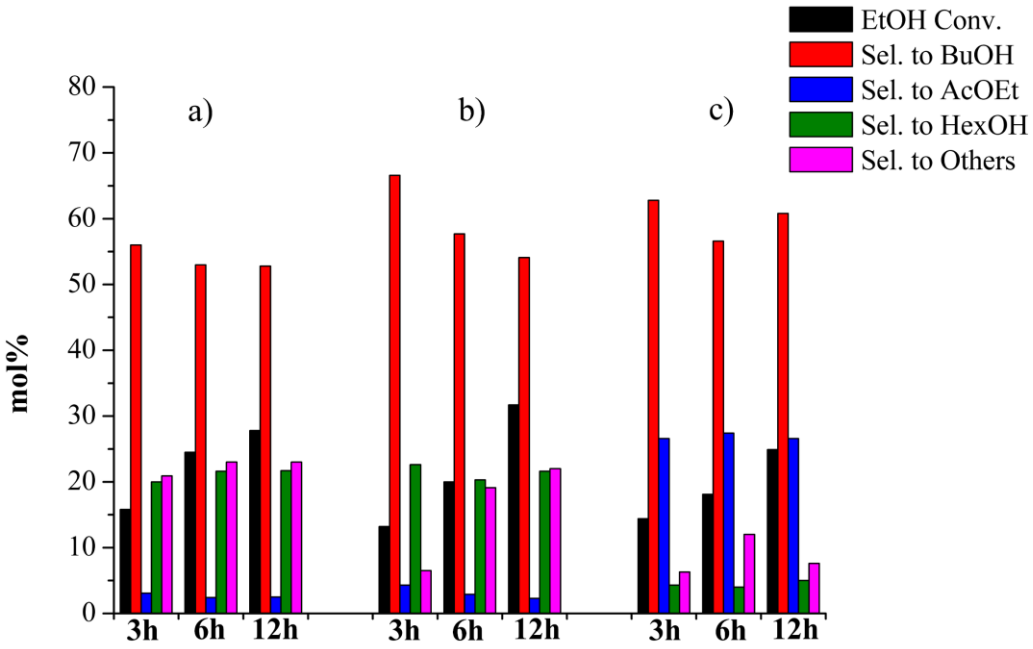


**Figure 4:** Influence of Cu loading on the catalytic performances of the different catalysts at temperature 215 °C, EtOH 893 mmol: a) Cu1.0 catalyst, Cu: 1 mmol (MgO 67,9 mmol); b) Cu2.8 catalyst, Cu: 2.68 mmol (MgO 65,9 mmol); c) Cu7.6 catalyst, Cu: 7.1 mmol, (MgO 59 mmol). Other products: 2-ethyl-1-hexanol, 1,1-diethoxy-ethane, ethyl butyrate, 2-ethyl-1-butanol, 1-octanol.

**Figure 5**

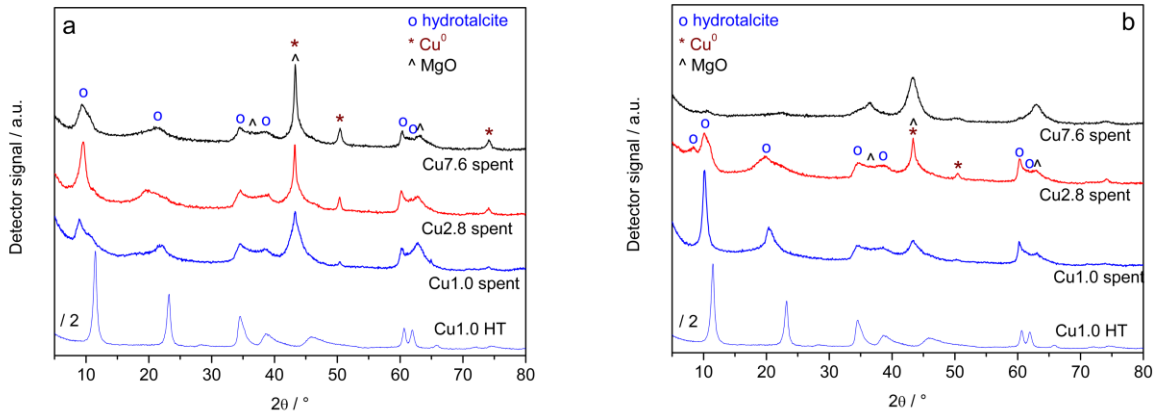


**Figure 5** a) Diffraction patterns of the spent catalysts Cu7.6, Cu2.8 and Cu1.0, together with diffraction pattern of the catalyst precursor Cu1.0 HT; b) Diffraction patterns of the spent pre-reduced catalysts Cu7.6, Cu2.8 and Cu1.0, together with the diffraction pattern of the catalyst precursor Cu1.0 HT.

**Figure 6**

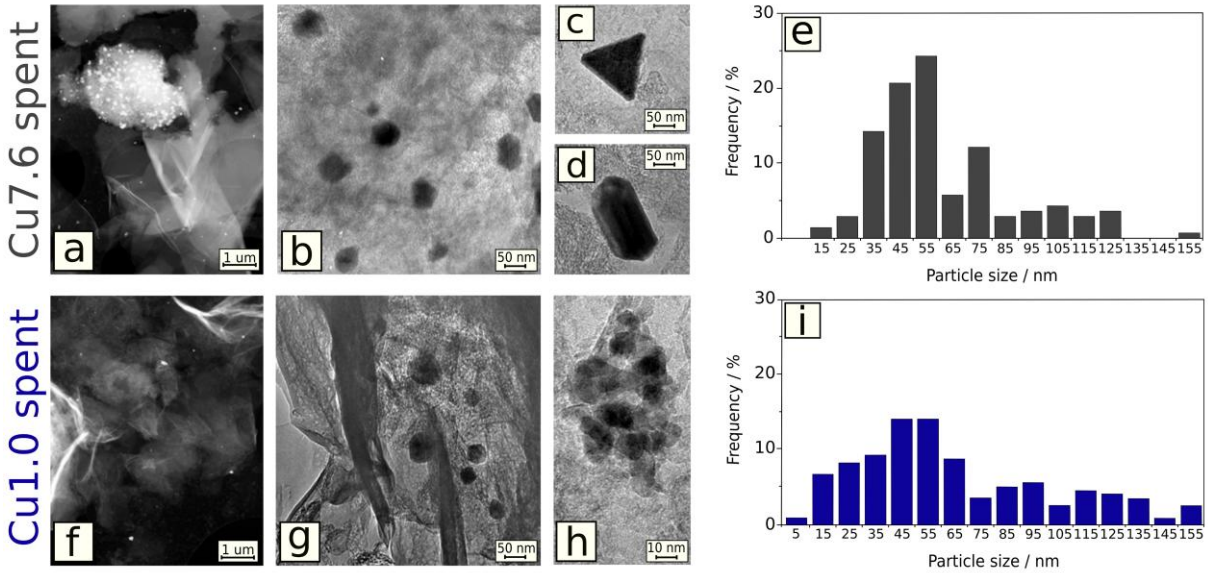


**Figure 6:** HRTEM characterization of Cu7.6 and Cu1.0 spent catalysts: HAADF/STEM images (a: Cu7.6; f: Cu1.0), HRTEM images (b, c, d: Cu7.6; g, h: Cu1.0) and particle size distributions (e: Cu7.6; i: Cu1.0).

**Figure 7**

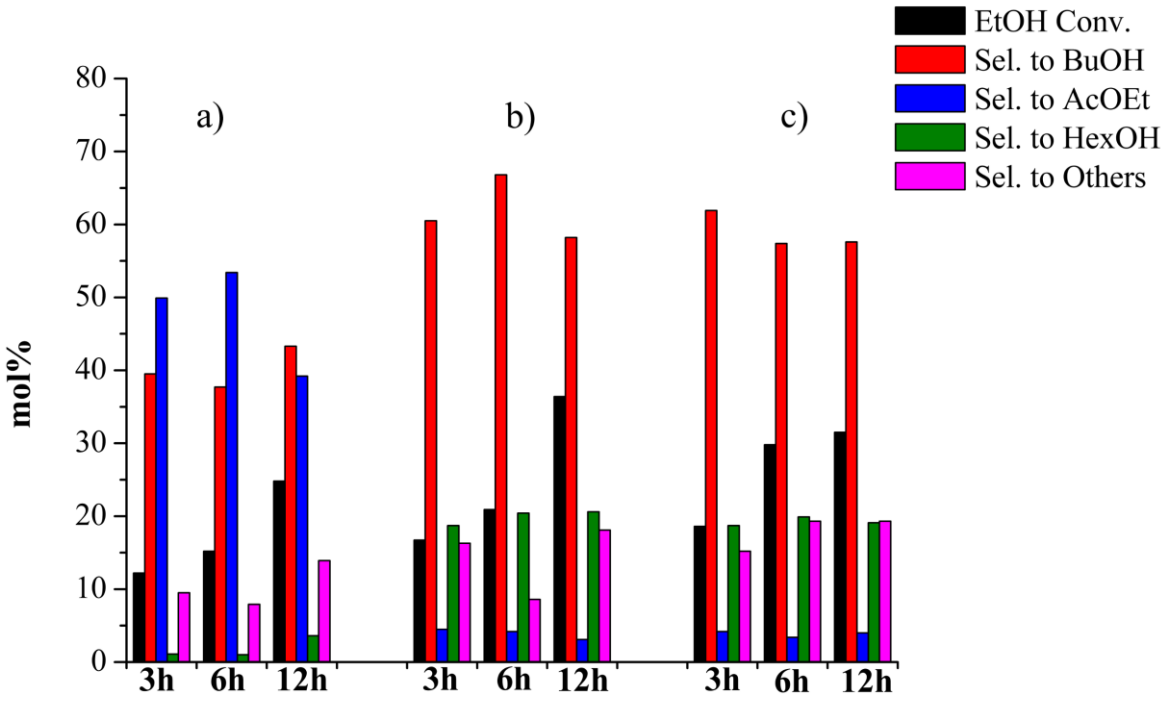


**Figure 7:** Influence of the pre-reduction step on the catalytic performances of the different catalytic systems in EtOH condensation at 215 °C, EtOH 893 mmol: a) Cu7.6 catalyst, Cu: 7.1 mmol (MgO: 59 mmol); b) Cu2.8 catalyst, Cu: 2.7 mmol (MgO: 63.4 mmol); c) Cu1.0 catalyst, Cu: 1 mmol (MgO: 68.3 mmol). Other products: 2-ethyl-1-hexanol, 1,1-diethoxy-ethane, ethyl butyrate, 2-ethyl-1-butanol, 1-octanol.

**Figure 8**

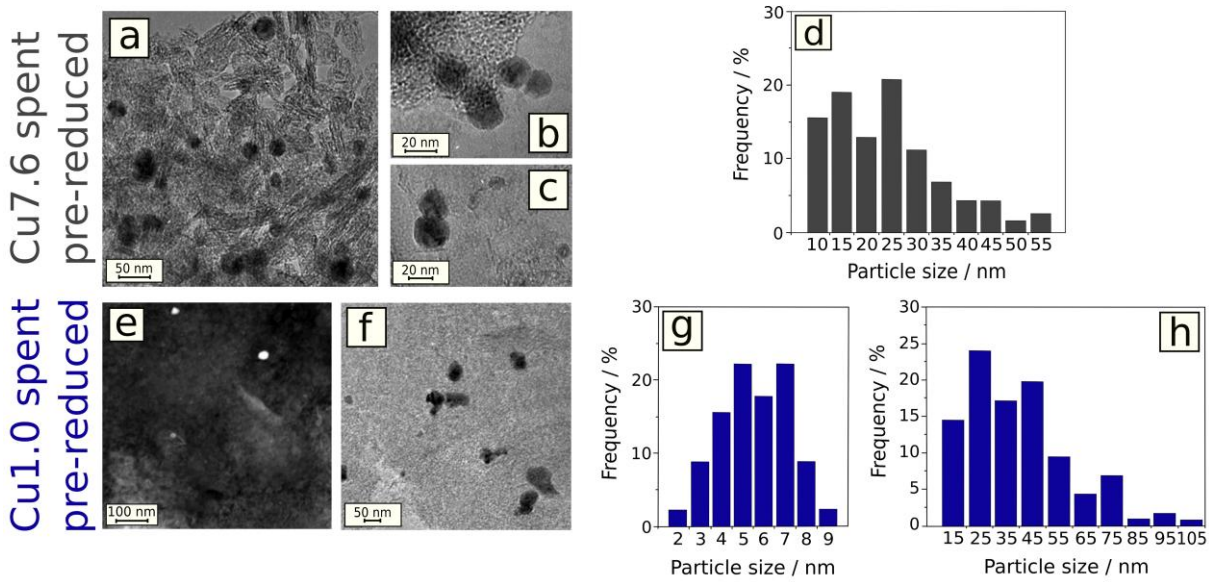


**Figure 8:** HRTEM characterization of Cu7.6 and Cu1.0 pre-reduced spent catalysts: HRTEM images (a, b, c: Cu7.6; f: Cu1.0), HAADF/STEM image (e: Cu1.0), and particle size distributions (d: Cu7.6; g, h: Cu1.0).

**Figure 9**

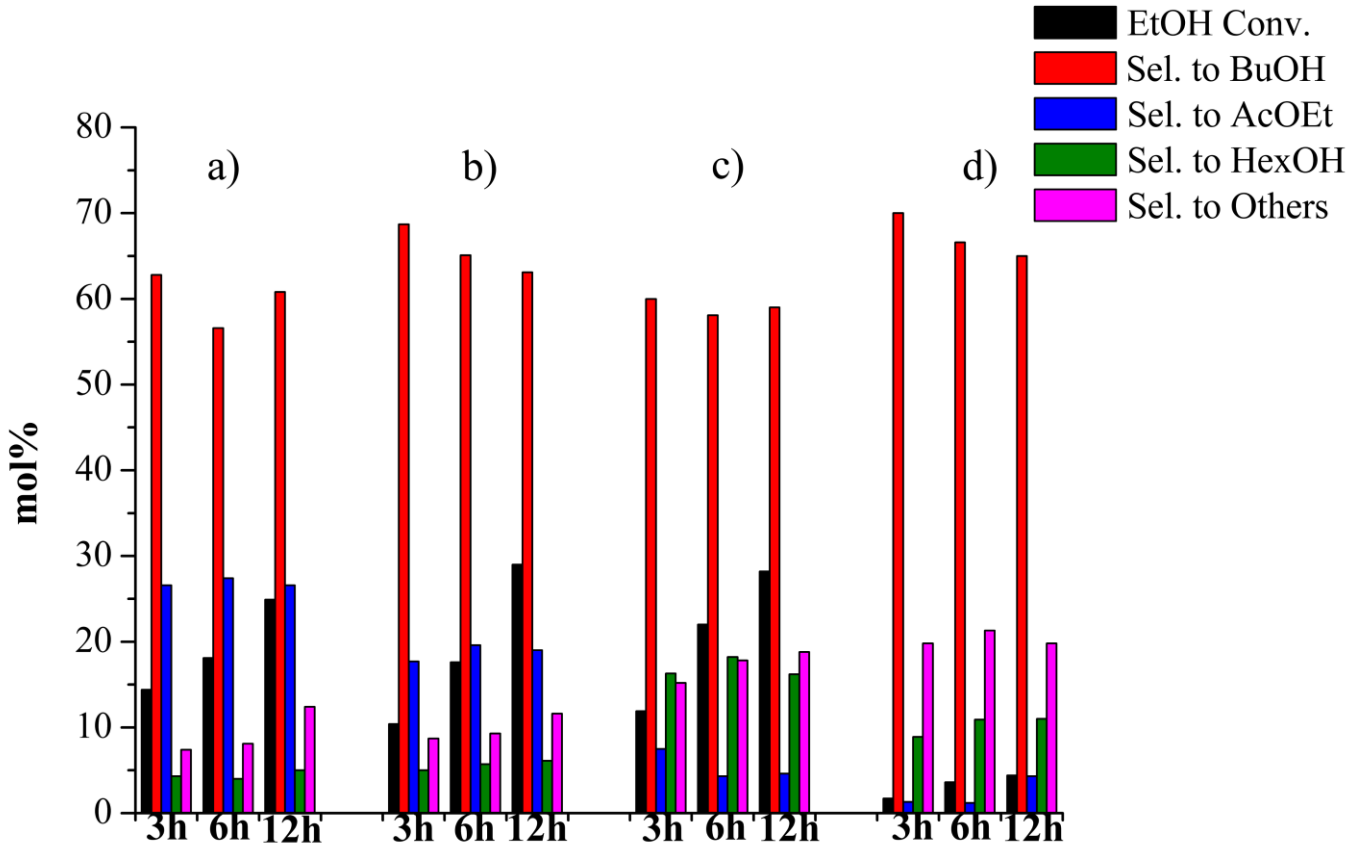


**Figure 9:** Influence of the addition of commercial MG Puralox on the catalytic performances of Cu7.6 catalyst at 215 °C, EtOH 893 mmol: a) Cu7.6 catalyst, Cu: 7.1 mmol (MgO 59 mmol), MG Puralox: absent; b) Cu7.6 catalyst, Cu: 3.8 mmol (MgO 31,6 mmol) MG Puralox: 34.2 mmol of MgO; c) Cu7.6 catalyst, Cu: 1 mmol (MgO 8.3 mmol) MG Puralox: 63 mmol of MgO; d) Cu7.6: absent; MG Puralox: 73.1 mmol of MgO. Other products: 2-ethyl-1-hexanol, 1,1-diethoxy-ethane, ethyl butyrate, 2-ethyl-1-butanol, 1-octanol.

**Figure 10**

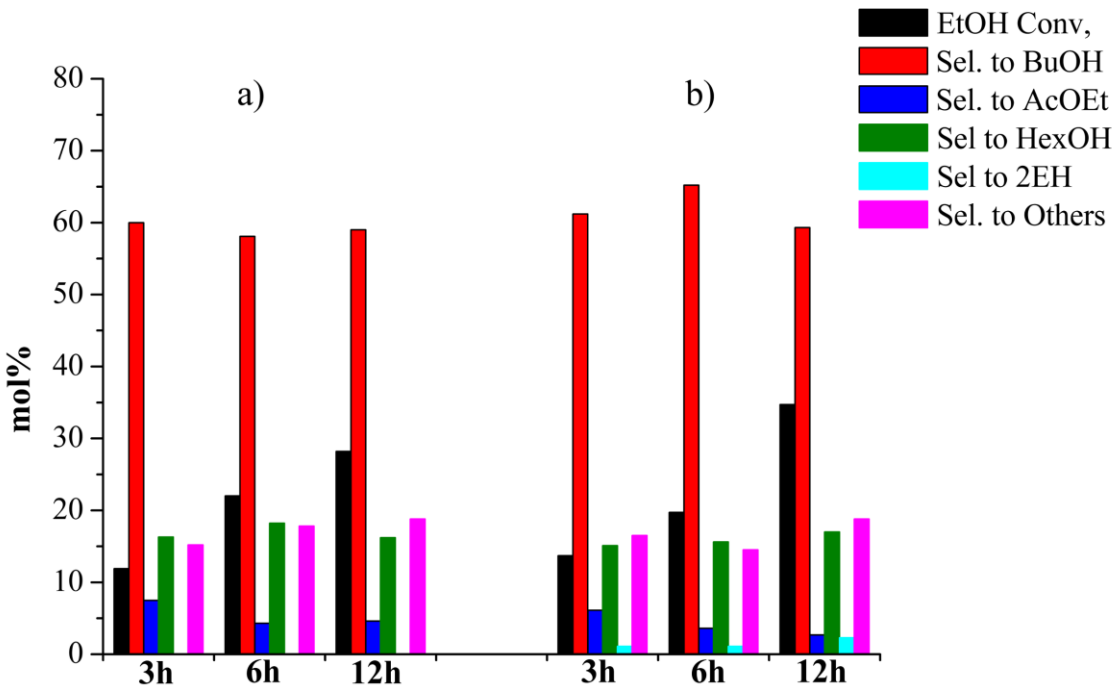


**Figure 10:** Influence of the presence of $MgSO_4$ on the catalytic performances of Cu7.6 at 215 °C, EtOH 893 mmol: a) Cu7.6 catalyst, Cu: 1 mmol, MgO 8.3 mmol, MG Puralox: 63 mmol of MgO; b) Cu7.6 catalyst, Cu: 1 mmol; MgO 8.3 mmol, MG Puralox: 63 mmol of MgO; $MgSO_4$: 3 g. Other products: 2-ethyl-1-hexanol, 1,1-diethoxy-ethane, ethyl butyrate, 2-ethyl-1-butanol, 1-octanol.

## Scheme 1

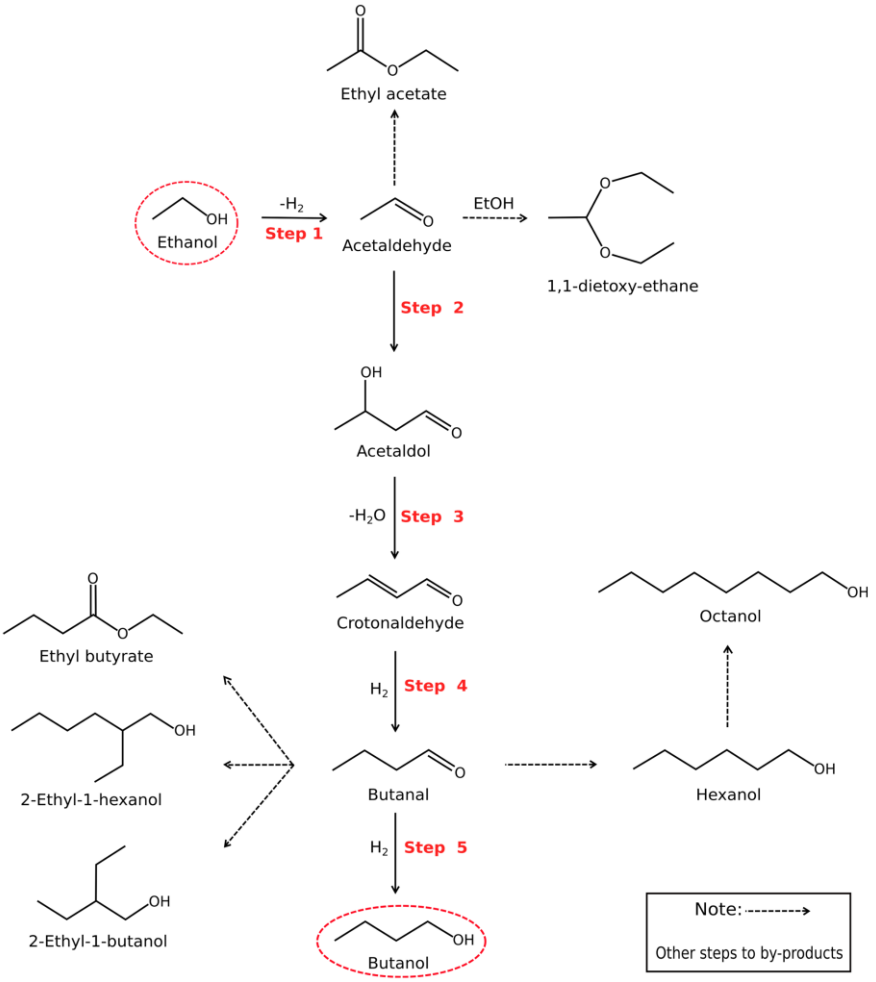


**Scheme 1:** Reaction network for Guerbet reaction.

**WORDS (manuscript, Tables, Figures and Scheme):7990**

# Tunable Cu-hydrotalcite derived mixed oxides for sustainable ethanol condensation to n-butanol in liquid phase

Patricia Benito[a*], Angelo Vaccari[a], Claudia Antonetti[b], Domenico Licursi[b], Nicola Schiarioli[a], Enrique Rodriguez-Castellón[c], Anna Maria Raspolli Galletti[b]*

[a]Dipartimento di Chimica Industriale "Toso Montanari", Università di Bologna, Viale Risorgimento 4, 40136, Bologna, Italy.

[b]Dipartimento di Chimica e Chimica Industriale, Università di Pisa, Via G. Moruzzi 13, 56124 Pisa, Italy.

[c]Departamento de Química Inorgánica, Facultad de Ciencias, Universidad de Málaga, 29071 Málaga, Spain

DECLARATION OF INTEREST: NONE

*Corresponding authors, e-mail: patricia.benito3@unibo.it; anna.maria.raspolli.galletti@unipi.it.

**Cover Letter**

UNIVERSITÀ DI PISA

DIPARTIMENTO DI CHIMICA E CHIMICA INDUSTRIALE

Via Giuseppe Moruzzi 13 - 56124 Pisa (Italy)

**Prof. Anna Maria Raspolli Galletti**
E-mail: anna.maria.raspolli.galletti@unipi.it

Pisa, 26th August 2018

Dear Editor,

please find enclosed our paper **"Tunable Cu-hydrotalcite derived mixed oxides for sustainable ethanol condensation to n-butanol in liquid phase**" for publication in ***"Journal of Cleaner Production".***

The condensation reaction is a catalytic strategy for upgrading lower alcohols to give valuable chemicals and energy-intensive green fuels. In particular, a smart catalytic route for the conversion of bioethanol into butanol and heavier alcohols is studied. This is a real hot topic since butanol, which can be obtained from biomass although no economically sustainable bioconversion processes are yet available, is a very promising gasoline additive, with better properties respect to ethanol and a green solvent. Although many homogeneous and heterogeneous catalysts have been proposed for this reaction, to date no promising performances have been achieved under moderate reaction conditions, working at subcritical temperatures in the liquid phase. The reaction has now been studied in the presence of Cu/Mg/Al hydrotalcite-derived mixed oxides. Different Cu/Mg/Al mixed oxides catalysts were synthesized, characterized and tested in the condensation tests carried out at temperatures 215-230 °C. Tailoring Cu-content in hydrotalcite-derived Cu/Mg/Al mixed oxides allowed to address the condensation towards BuOH formation with the best performances up to now reported working in the liquid phase.

According to the above reasons, we think that this paper is of relevant interest to many researchers in the field of new cleaner routes for bioalcohols production. This submission is original, it is not under consideration for publication elsewhere and all the authors are aware of the submission and agree to its publication. The English form has been revised by a native tongue speaker with expertise in the field.

Thanking you for kindly considering our manuscript for publication, I send you my best personal regards.

Sincerely yours,

Anna Maria Raspolli Galletti

**Graphical Abstract**

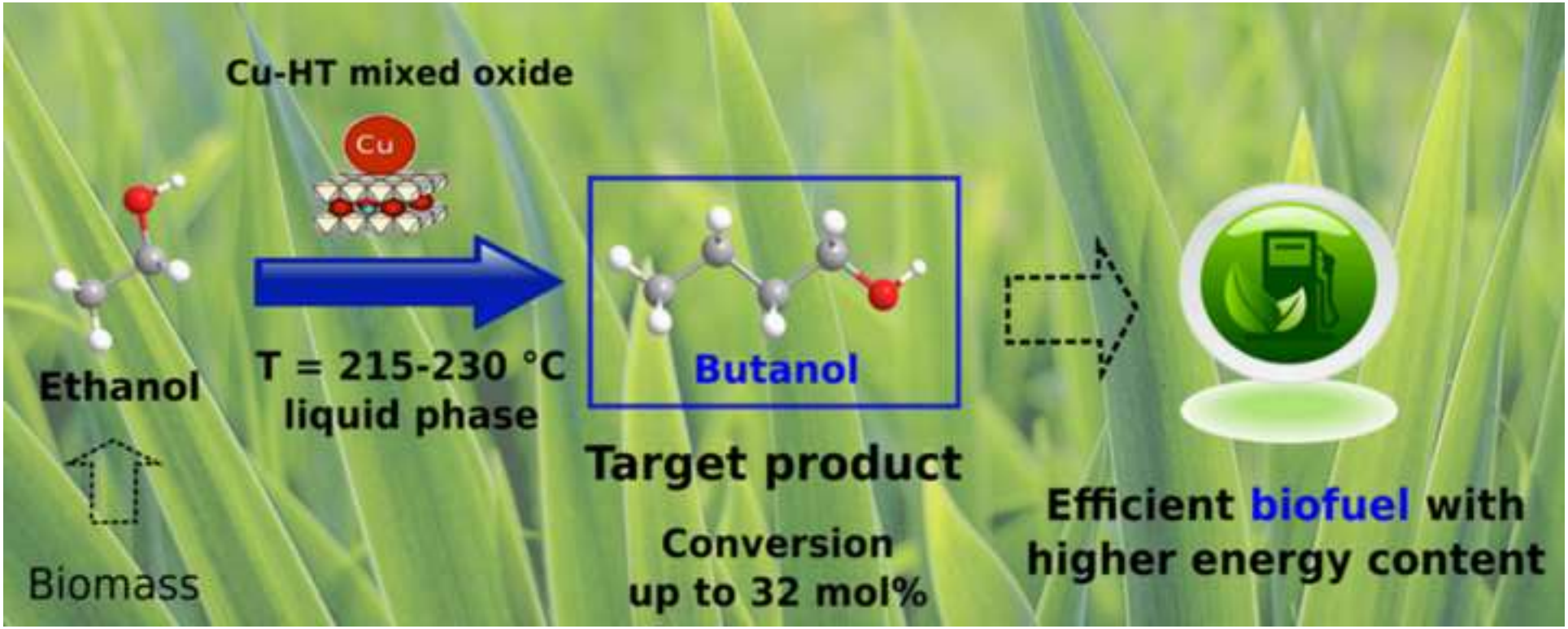

## Highlights

- BuOH was synthesized by condensation of ethanol in liquid phase.
- Different Cu/Mg/Al hydrotalcite-derived mixed oxides were employed as catalysts.
- Tailoring Cu-content allows us to address the reaction toward BuOH formation.
- Characterization of catalysts enables to establish structure-performance trends.
- Conversion up to 32.0 mol % with selectivity to BuOH of 53 mol% were ascertained.

**Figure1**

**Click here to download high resolution image**

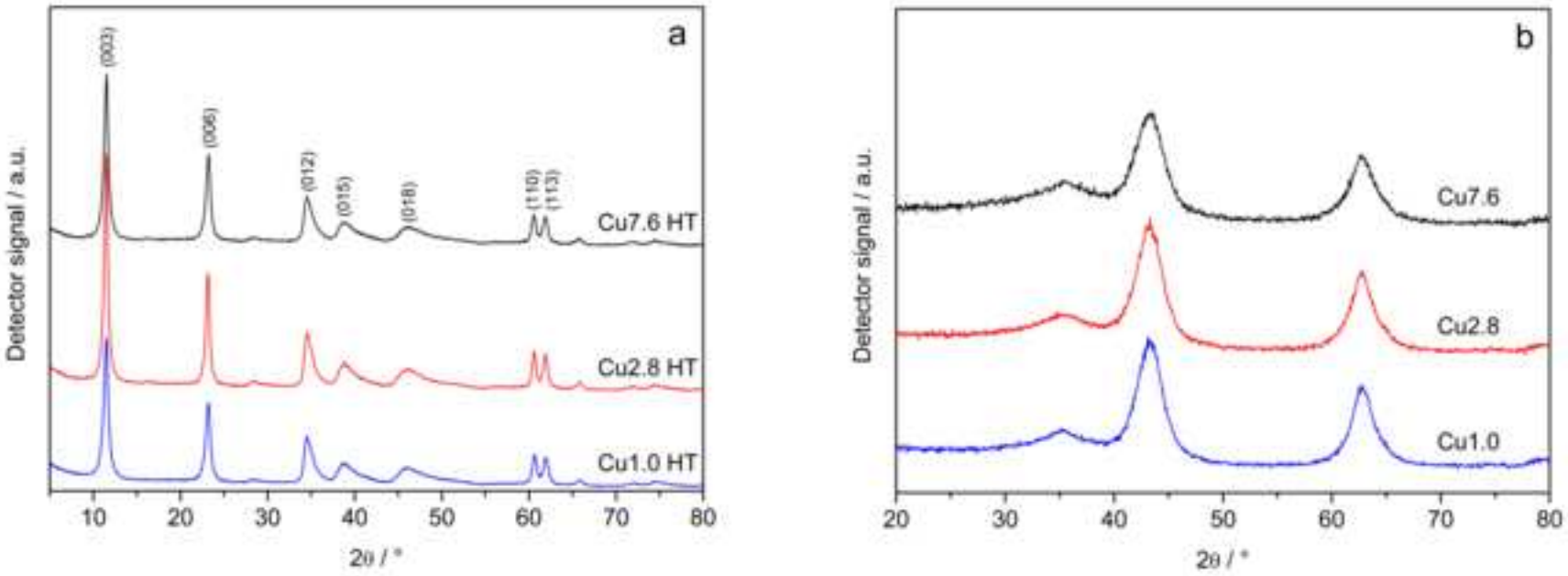

Figure2
Click here to download high resolution image

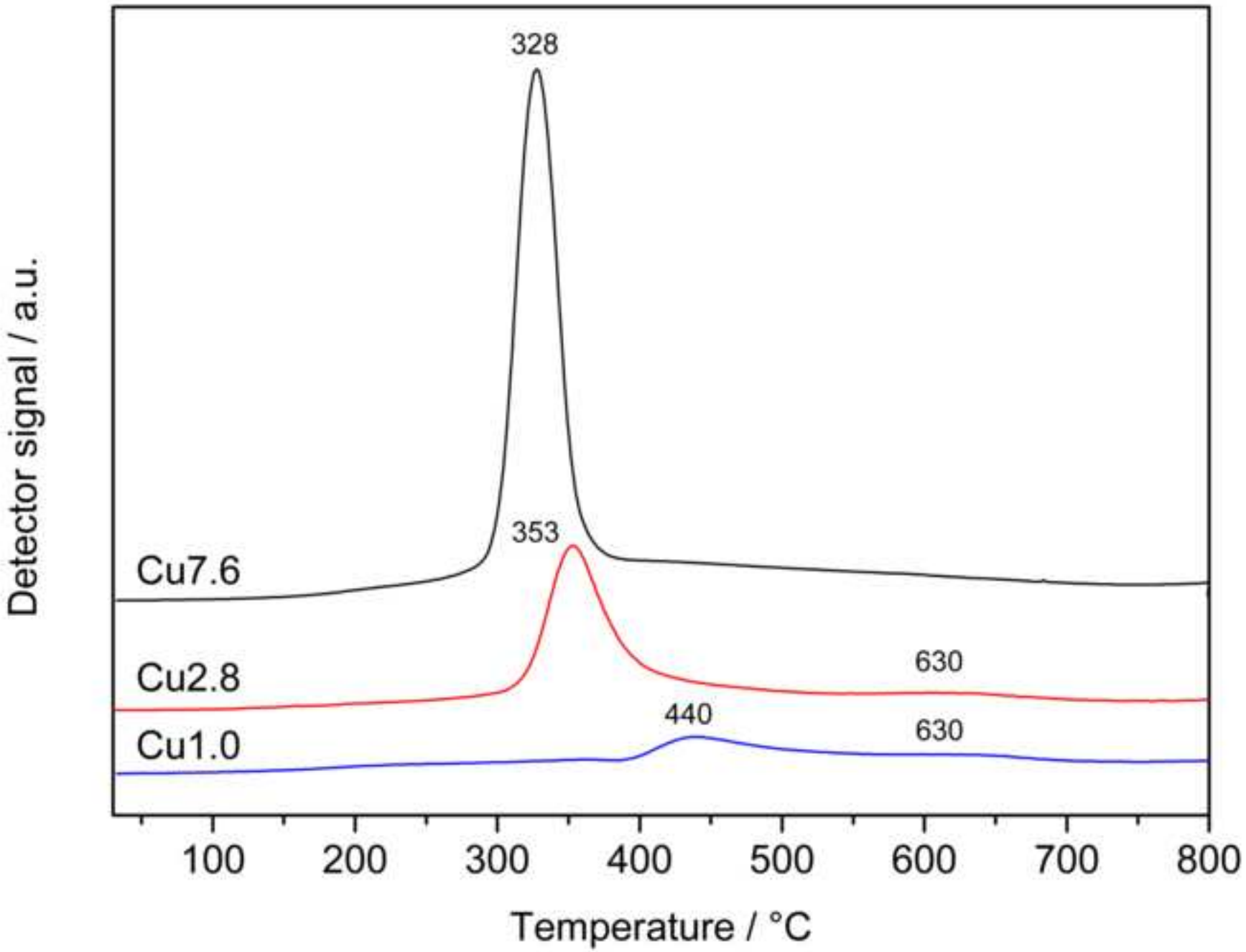

Figure3

Click here to download high resolution image

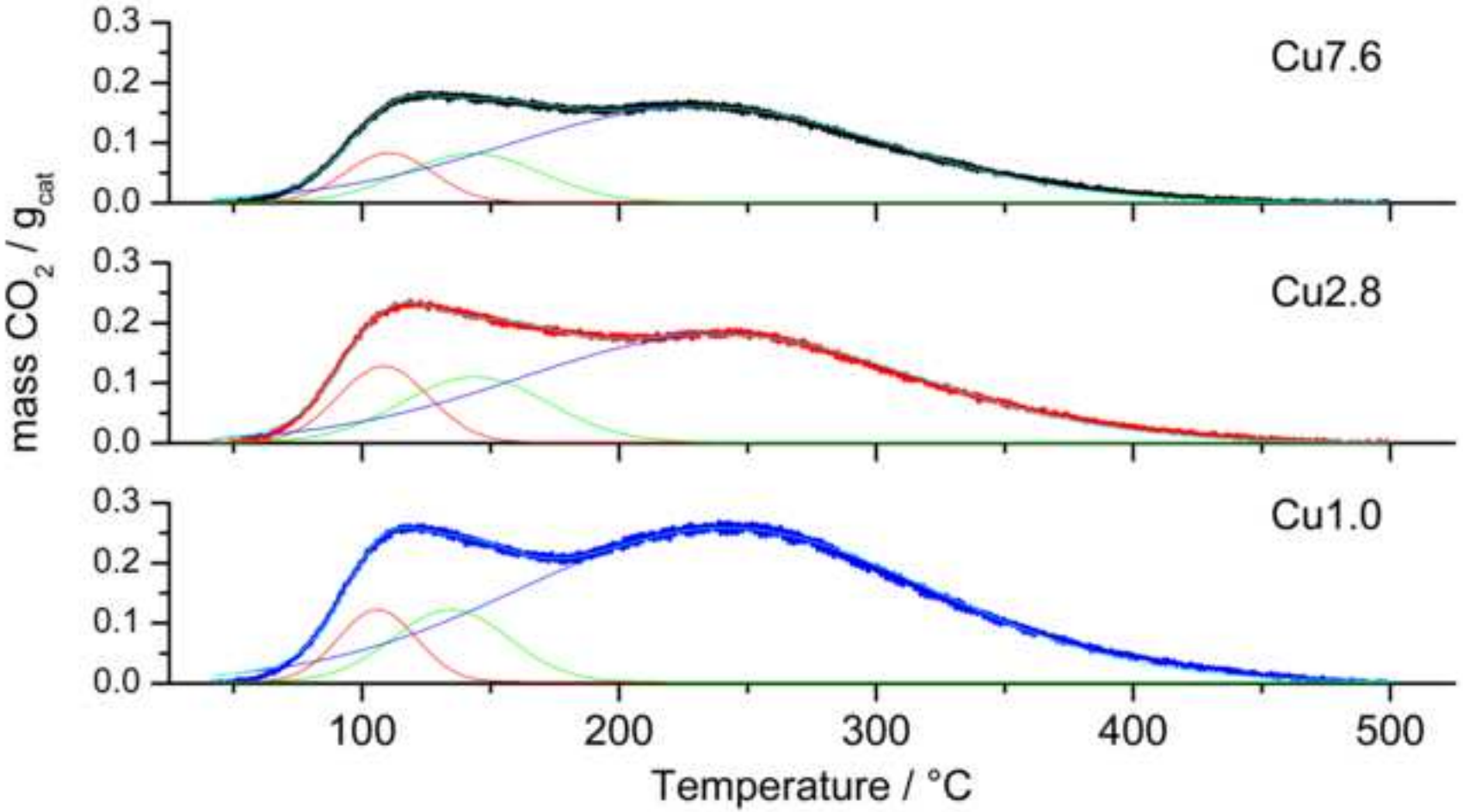

Figure4

Click here to download high resolution image

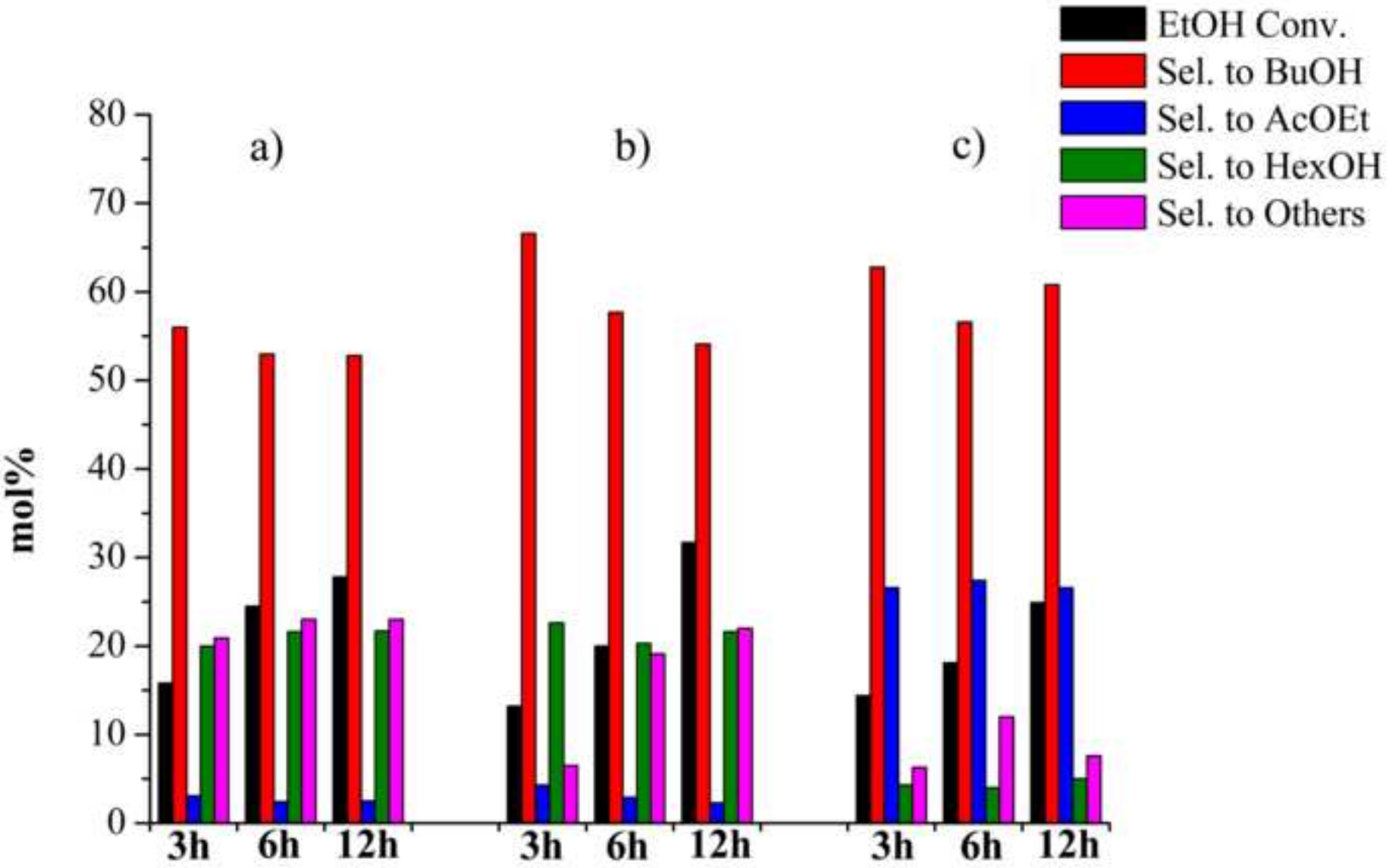

Figure5

Click here to download high resolution image

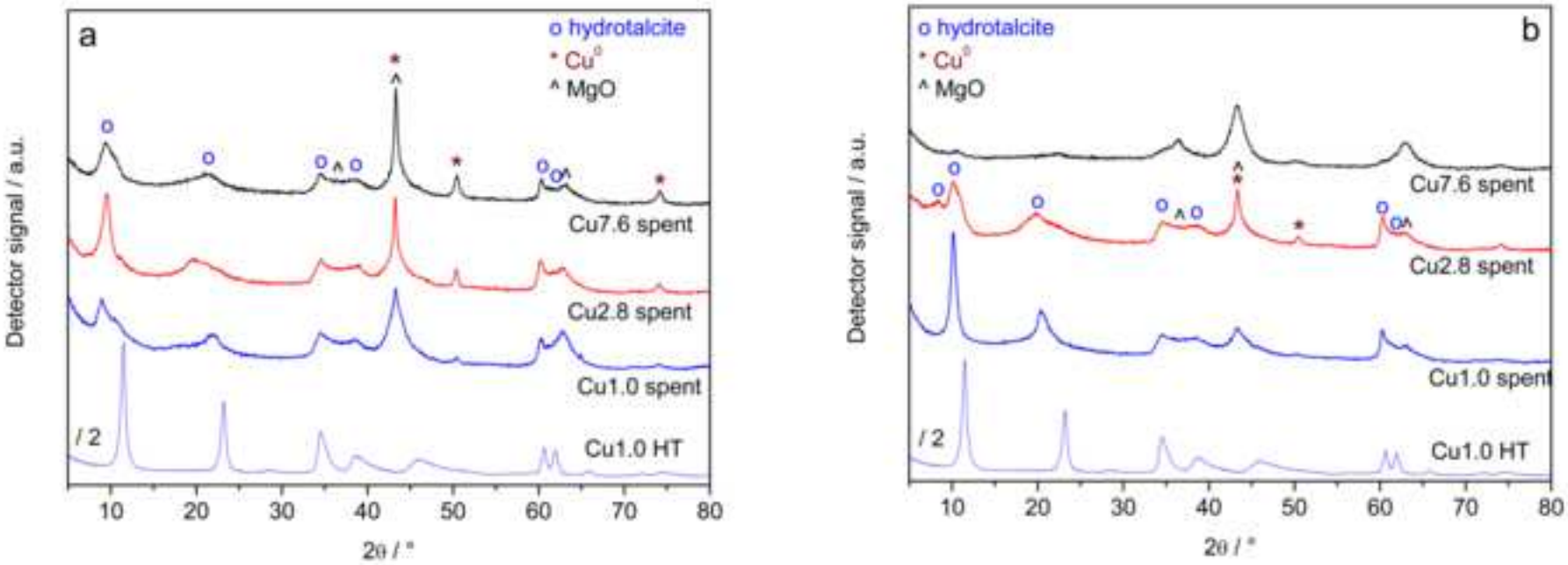

Figure6

Click here to download high resolution image

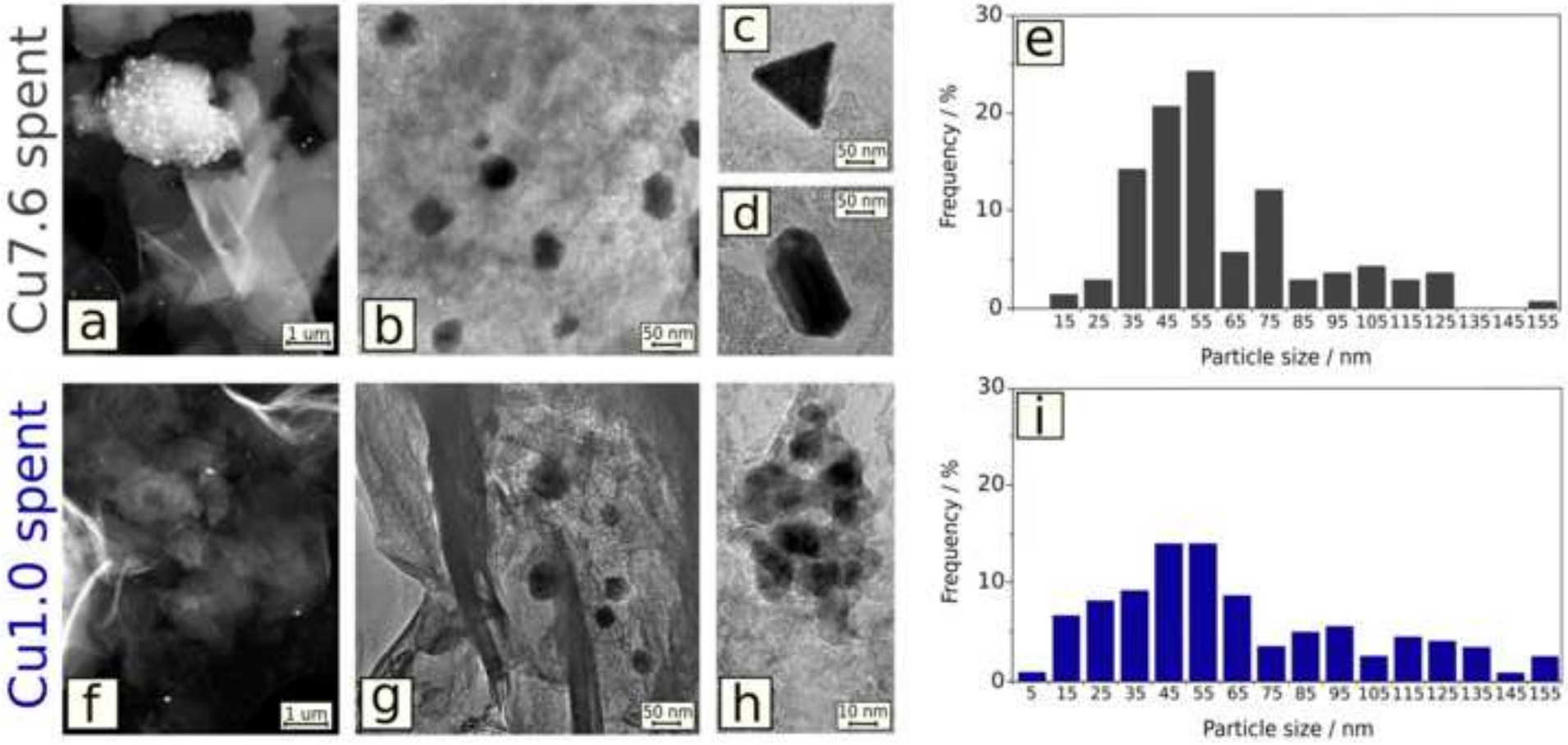

Figure7

Click here to download high resolution image

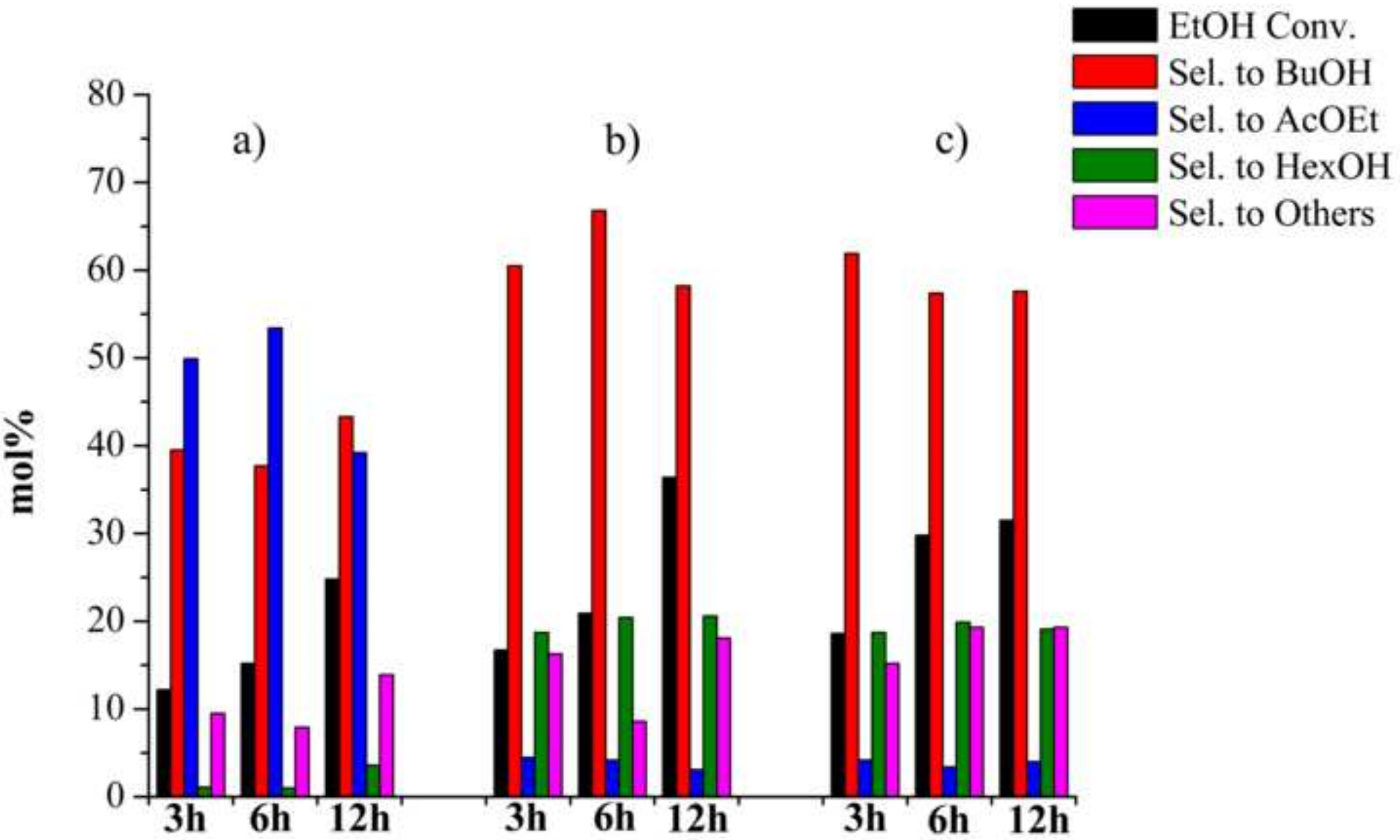

Figure8

Click here to download high resolution image

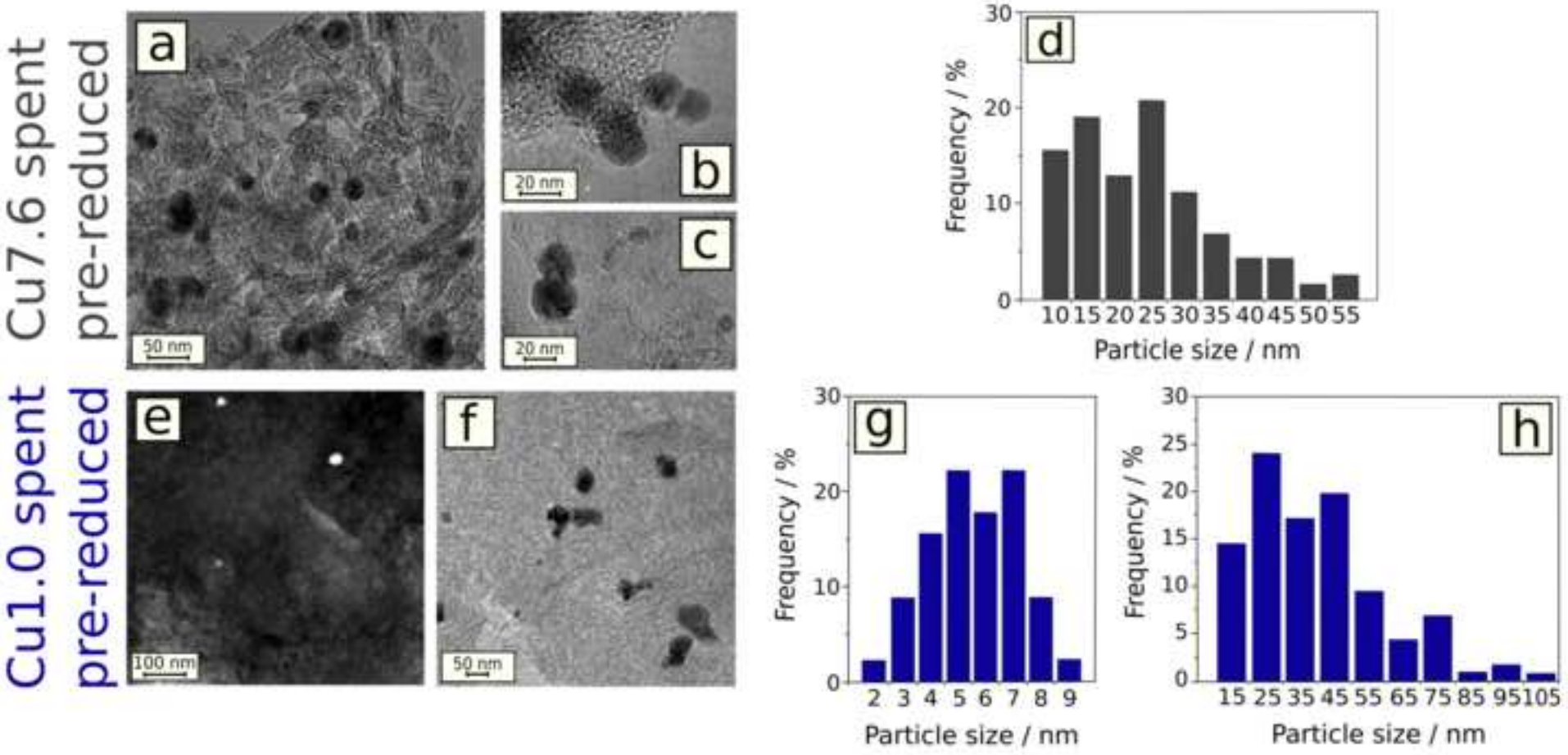

Figure9

Click here to download high resolution image

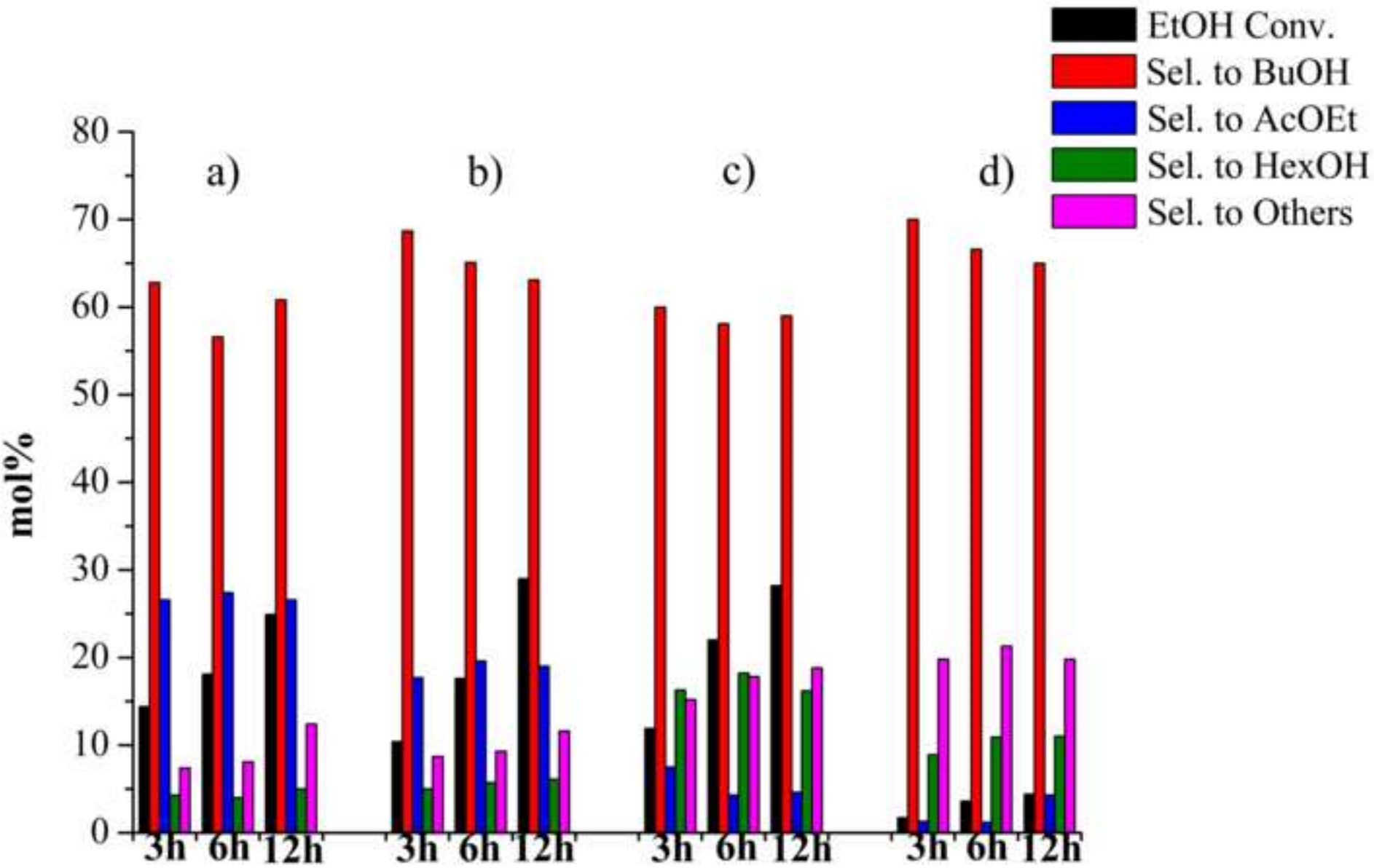

Figure10

Click here to download high resolution image

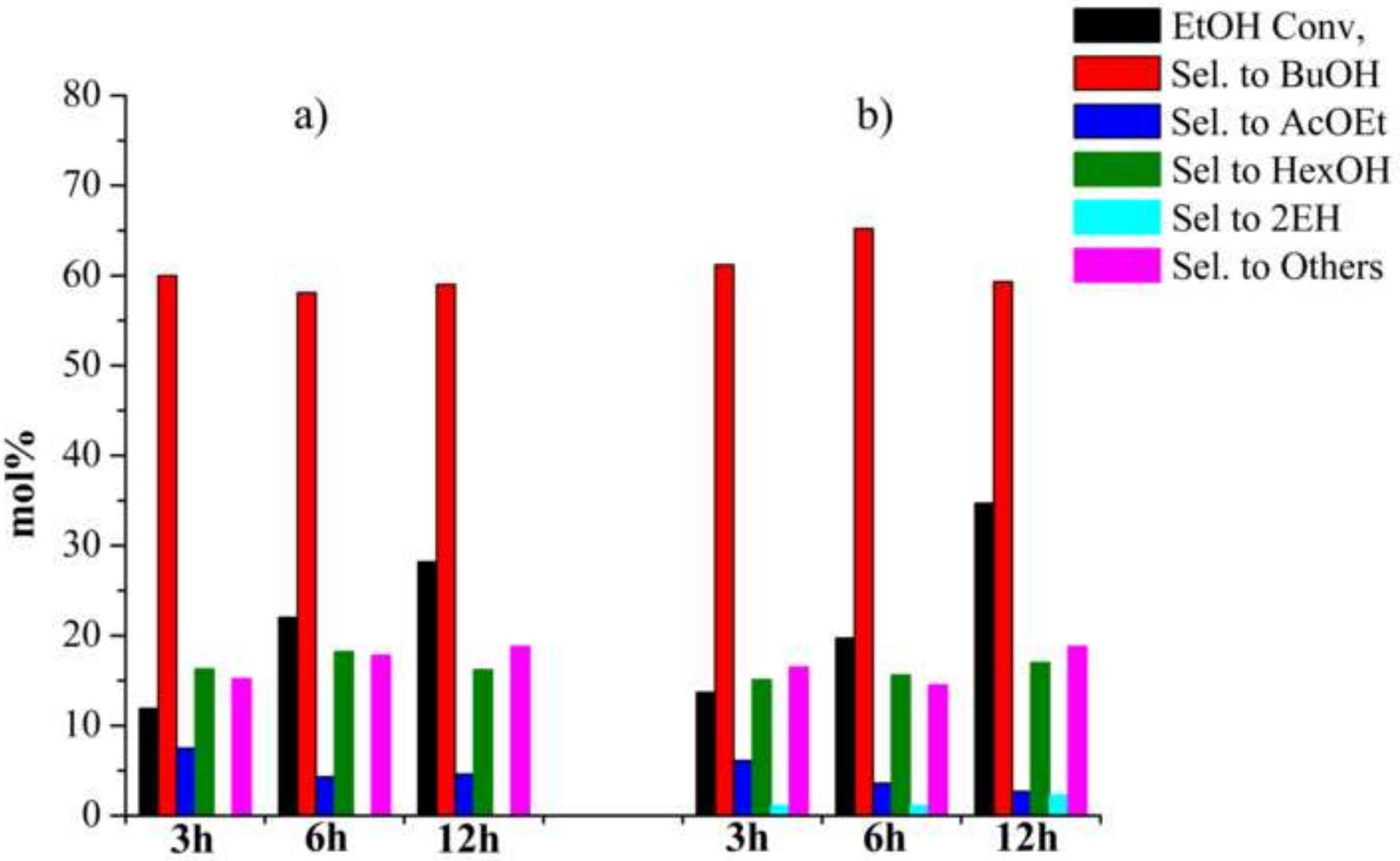

**Scheme1**

**Click here to download high resolution image**

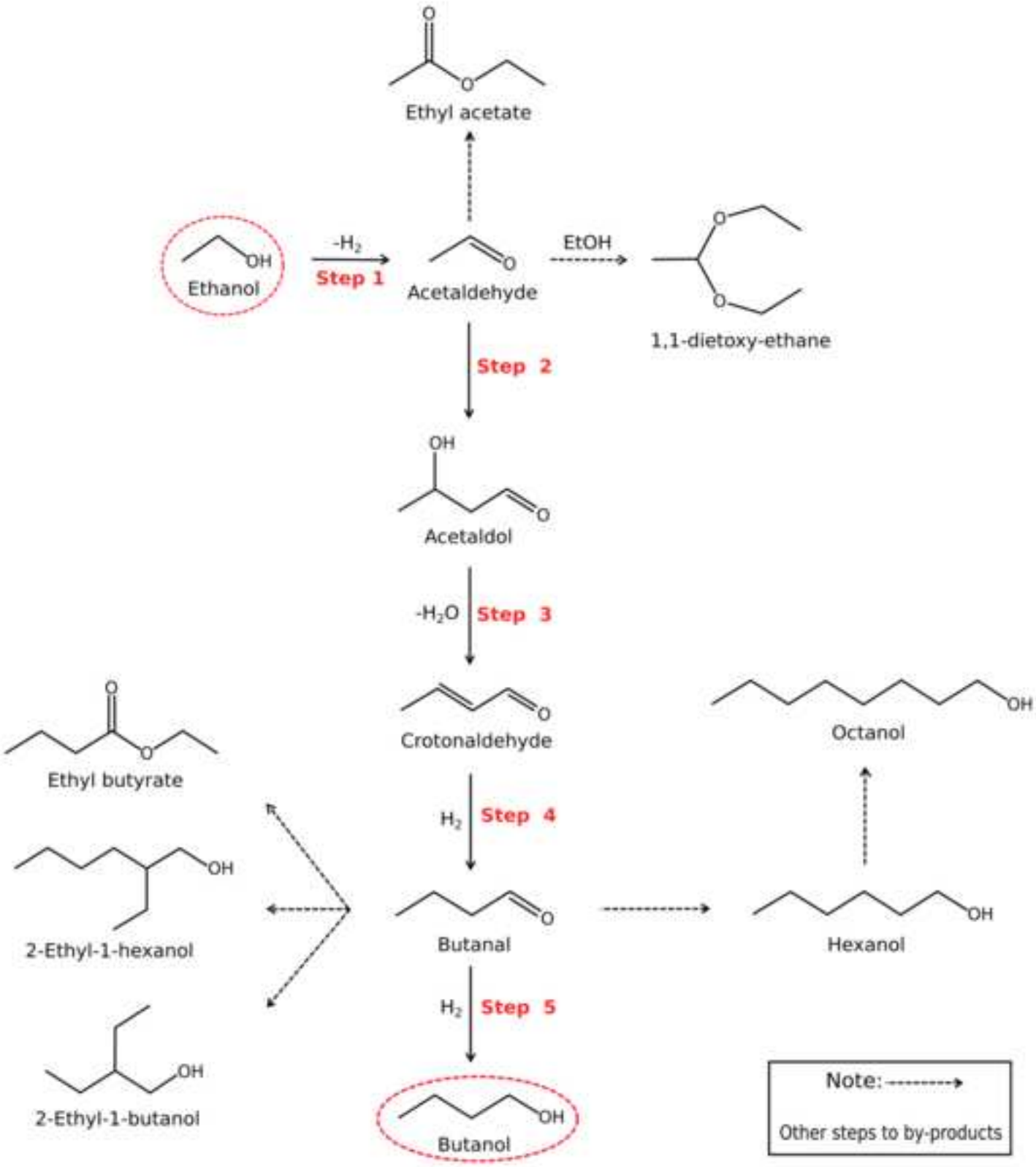

**Supplementary Interactive Plot Data (CSV)**

**Click here to download Supplementary Interactive Plot Data (CSV): Supplementary Information.pdf**

# Supplementary Information

**Figure S1:** HRTEM image of Cu1.0-HT

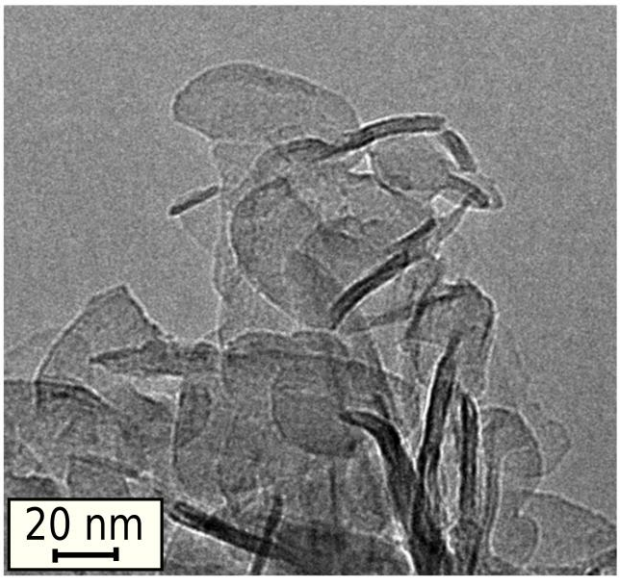


**Figure S2:** XPS spectra of $Cu2p_{3/2}$ core level acquired from spent Cu7.6 catalyst not pre-reduced (a) and pre-reduced (b)

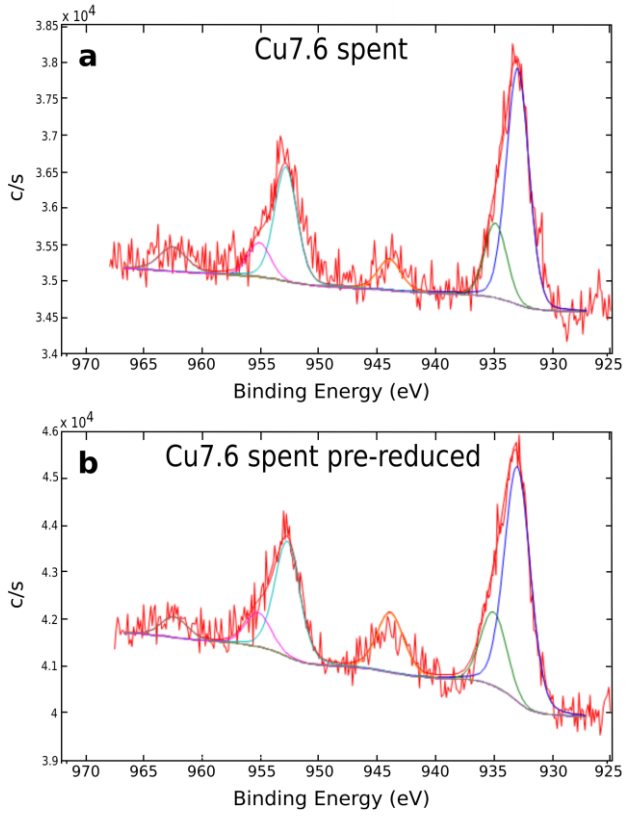

**Figure S3:** XPS spectra of $Cu2p_{3/2}$ core level acquired from spent Cu1.0 catalyst not pre-reduced (a) and pre-reduced (b)

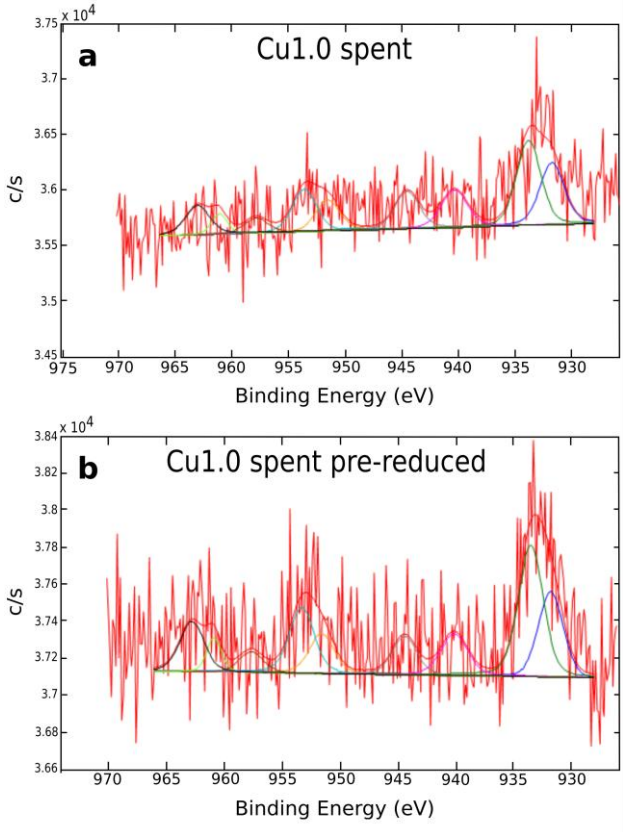


**Figure S4:** Diffraction pattern of Cu7.6 catalyst reduced in MeOH at 180°C under 5 MPa $H_2$

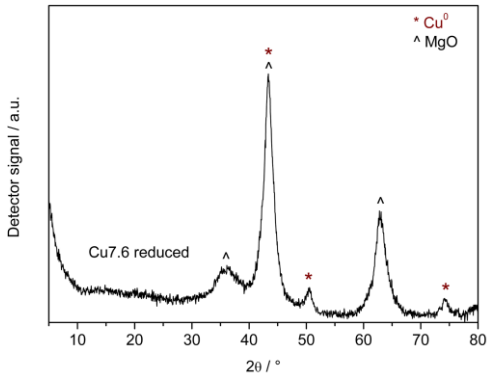

**Figure S5:** HRTEM characterization of Cu7.6 catalyst reduced in MeOH at 180°C under 5 MPa $H_2$. a: HRTEM image of a region with Cu particles in the 10-50 nm range (a1). b: HAADF/STEM image of a region with Cu particles in the 2-8 nm range (b1).